Journal of Quantitative Spectroscopy & Radiative Transfer 235 (2019) 217–231

Contents lists available at ScienceDirect

Journal of Quantitative Spectroscopy & Radiative Transfer

journal homepage: www.elsevier.com/locate/jqsrt

Ab initio MCDHF/RCI and semi-empirical HFR calculations of transition probabilities and oscillator strengths in Xe XI

E. Bokamba Motoumba[a], S. Enzonga Yoca[a,b], P. Quinet[c,d], P. Palmeri[c,*]

[a] Faculté des Sciences et Techniques, Université Marien Ngouabi, BP 69, Brazzaville, Congo
[b] Conseil Africain et Malgache pour l'Enseignement Supérieur – CAMES, 01 BP 134, Ouagadougou 01, Burkina Faso
[c] Physique Atomique et Astrophysique, Université de Mons – UMONS, Mons B-7000, Belgium
[d] IPNAS, Université de Liège, Liège B-4000, Belgium

A R T I C L E I N F O

Article history:
Received 5 February 2019
Revised 13 May 2019
Accepted 5 July 2019
Available online 9 July 2019

Keywords:
Atomic structure
Transition probabilities
Oscillator strengths
Xe XI spectrum

A B S T R A C T

The atomic structure of ten-times ionized xenon (Xe XI) has been computed by two independent methods, i.e. the *ab initio* relativistic multiconfiguration Dirac–Hartree–Fock (MCDHF) approach within the relativistic configuration interaction (RCI) approximation and the semi-empirical pseudo-relativistic Hartree–Fock (HFR) method. The transition probabilities and oscillator strengths of the $4d^8 - (4p^5 4d^9 + 4d^7 5p + 4d^7 4f)$ transition array have been determined in both models and allowed us to estimate their accuracy taking into account both the gauge agreements and the cancellation effects on the line strengths. It has been found that core – core and core – valence correlations through the explicit inclusion of single- to triple-hole 4p-subshell configurations in our RCI model systematically decrease the transition rates by about 20% for the strong lines (with log gf > 0) with respect to our HFR values that did not consider those effects. Further opening of the core shells has also been investigated and did not give rise to significant systematic change on the transition probabilities.

1. Introduction

The spectrum of Xe XI is of great interest for the development of new extreme ultraviolet (EUV) light sources for application to lithography [1]. This is due to its strong line emissivity in the 111 – 113 Å wavelength band where the reflection coefficient of Ru/Be and Mo/Be mirrors peaks two times higher than a Mo/Si mirror operating in the 134 – 136 Å emission band of tin ions [2].

Another noticeable application concerns fusion energy [3-5]. Noble gases can be injected into nuclear fusion reactors, conditioned in solid pellets, for both plasma diagnostics and fuel introduction. In particular, xenon could be pumped out, without leaving residuals on plasma facing material and could therefore be recycled in subsequent discharges in ITER. In addition, it would be stripped to helium-like ions in the hottest part of the confined plasma. In that context, it would be thus crucial to have the knowedge of the spectroscopic parameters from all ionization stages of xenon including Xe XI in order to model the plasma and analyze the spectra to extract the physical conditions inside the tokamaks such as temperatures and densities.

Previous spectroscopic studies regarding Xe XI include those of Churilov et al. [6,7]. These authors recorded the high-resolution spectrum of xenon from a low-inductance vacuum spark between 100 and 200 Å using the 10.7-m grazing-incidence spectrograh at the National Institute of Standards and Technology (NIST). About 200 lines belonging to the electric dipole (E1) transition arrays $4d^8 - (4p^5 4d^9 + 4d^7 5p + 4d^7 4f)$ of Xe XI were classified with the help of Hartree–Fock calculations and orthogonal parameters. All the levels of the even-parity configuration $4d^8$ along with 123 levels belonging to the group of strong interacting odd-parity configurations $4p^5 4d^9$, $4d^7 5p$ and $4d^7 4f$ were determined. Moreover, the calculated transition probabilities were also reported for the classified lines.

A more recent work is due to Shen et al. [8] who computed the energy levels, transition probabilities, and electron impact collision strengths using the relativistic configuration interaction (RCI) method and the distorted wave approximation implemented in the Flexible Atomic Code (FAC) [9]. The transition rates were given for dipole allowed (E1) transitions between the first 400 fine structure levels of their model. They compared their calculated rates with the Hartree–Fock values of Churilov et al. [7] for 31 strong lines in order to assess their accuracy and concluded that they were better than 20%.

* Corresponding author.
E-mail address: patrick.palmeri@umons.ac.be (P. Palmeri).

https://doi.org/10.1016/j.jqsrt.2019.07.006
0022-4073/

The present analysis aims at investigating further the correlation effects on the radiative properties of Xe XI and providing assessed accurate oscillator strengths and transition probabilities for lines of interest in lithography and fusion energy. In that purpose, two independent atomic structure computational approaches, i.e. the *ab initio* relativistic multiconfiguration Dirac–Hartree–Fock (MCDHF) method within the relativistc configuration interaction (RCI) approximation, and the semi-empirical pseudo-relativistic Hartree–Fock (HFR) approach, have been used to determine the transition rates of the $4d^8 - (4p^5 4d^9 + 4d^7 5p + 4d^7 4f)$ E1 transition array of Xe XI located in the EUV spectral range. In addition, the configuration interaction (CI) expansions have been significatively extended compared to the few previous studies [7,8]. In the following section, we present the models used. Section 3 is dedicated to the discussion of our results and we finally draw our conclusions in Section 4.

2. Atomic structure and transition rate calculations

2.1. Ab initio MCDHF/RCI method

In order to calculate the oscillator strengths of the E1 transition arrays $4d^8\ J^\Pi = 0$–$4 - (4p^5 4d^9 + 4d^7 5p + 4d^7 4f)\ J^\Pi = 0^\circ - 5^\circ$, the fully relativistic multiconfiguration Dirac–Hartree–Fock (MCDHF) method [10] was used as implemented in the GRASP2K atomic structure computer package [11]. In this method [10], the atomic state function (ASF), Ψ, is represented by a superposition of configuration state functions (CSF), Φ, with the same parity, Π, total angular momentum, and total magnetic quantum numbers, J and M_J, forming a basis set of the representation, $\{\Phi_k\}$, as

$$\Psi\left(\Pi J M_J\right) = \sum_k c_k \Phi_k\left(\gamma_k \Pi J M_J\right) \tag{1}$$

where $\{c_k\}$ are the mixing coefficients, γ_k represents all the other quantum numbers needed to univoquely specify the CSF built from one-electron spin-orbitals, $\phi_{n\kappa m}(r, \theta, \varphi)$, of the form:

$$\phi_{n\kappa m}(r,\theta,\varphi) = \frac{1}{r}\begin{pmatrix} P_{n\kappa}(r)\chi_{\kappa m}(\theta,\varphi) \\ iQ_{n\kappa}(r)\chi_{-\kappa m}(\theta,\varphi)\end{pmatrix}. \tag{2}$$

$P_{n\kappa}(r)$ and $Q_{n\kappa}(r)$ are, respectively, the large and the small radial components of the wave functions, and the angular functions $\chi_{\kappa m}(\theta, \varphi)$ are the spinor spherical harmonics [10]. The quantum number κ is given by:

$$\kappa = \pm\left(j + \frac{1}{2}\right), \tag{3}$$

where $\kappa = -(j + 1/2)a$, with a defined so that

$$l = j - \frac{1}{2}a;\ a = \pm 1. \tag{4}$$

The radial functions $P_{n\kappa}(r)$ and $Q_{n\kappa}(r)$ are numerically represented on a logarithmic grid and are required to be orthonormal within each κ symmetry. In the MCDHF variational procedure, the radial functions and the expansion coefficients c_k are optimized to self-consistency [10, 12].

In this work, the spectroscopic configurations, i.e. $4s^2 4p^6 4d^8$ $J^\Pi = 0-4$, $4s^2 4p^5 4d^9$ $J^\Pi = 0^\circ - 5^\circ$, $4s^2 4p^6 4d^7 5p$ $J^\Pi = 0^\circ - 5^\circ$ and $4s^2 4p^6 4d^7 4f$ $J^\Pi = 0^\circ - 5^\circ$, were used as reference configurations to generate all the CSFs forming the basis set by single and double electron excitations to the following active set of orbitals: {4p, 4d, 4f, 5s, 5p, 5d, 5f}. This led to form a basis of 1 502 358 CSFs. This ensures that important core–valence and valence–valence correlations are taken into account in our model. The configuration space was then reduced in order to render a relativistic configuration interaction (RCI) calculation feasible by keeping the CSFs that directly interact with at least one of the 295 spectroscopic CSFs [13]. This generated a basis of 1 295 454 CSFs. The orbitals were then optimized using the extended average level (EAL) option of GRASP2K [10, 11] in separated Dirac–Hartree–Fock (DHF) calculations that included all the states of one non-relativistic electronic configuration as follows:

- all the core orbitals, i.e. 1s to 3d, along with the orbitals 4s, 4p and 4d were obtained by an EAL DHF optimization on the ground configuration $4d^8$;
- the orbitals 4f, 5s, 5p, 5d and 5f were optimized on the configurations $4d^7 4f$, $4d^7 5s$, $4d^7 5p$, $4d^7 5d$ and $4d^7 5f$ respectively.

Finally, the high-order relativistic effects, i.e. the Breit interaction, QED self-energy and vacuum polarization effects [1], were incorporated in the RCI step of the GRASP2K package [2]. This model will be referred as to RCI-CV(4p).

In order to test the effects of opening further the electronic core sub-shells, a second RCI model labelled RCI-CV(4 s,4p) that differs from our RCI-CV(4p) model in the opening the 4 s subshell allowing single and double excitation from it and in limiting the symmetries of the odd ASFs to $J^\Pi \le 2^\circ$ and that of the even ASFs to $J^\Pi \le 3$. The latters meant to keep the dimension of the CSF basis (758 761 CSFs) manageable.

As a check of valence correlation with atomic orbitals outside the $n = 5$ Layzer complex, two additional RCI models were carried out. The first one, labelled RCI-V(5f), differed from our RCI-CV(4p) model in no more considering the 4p orbital as active in the CSF generation by single and double electron excitations from the same reference configurations. This resulted in a basis of 168 092 CSFs. In the second one labelled RCI-V(6f), the RCI-V(5f) model was extended in adding further the 6s, 6p, 6d and 6f orbitals to the active set. This generated 450 802 CSFs. The $n = 6$ orbitals were separately optimized on the configurations $4d^7 6s$, $4d^7 6p$, $4d^7 6d$ and $4d^7 6f$ following a similar procedure as used in our RCI-CV(4p) model.

The final transition amplitudes were computed in both the Babushkin and the Coulomb gauges, the relativistic equivalents of the length and velocity gauges respectively. The gauges agreement for a given transition provides a measure of the accuracy of its transition probability although the former condition is necessary but not sufficient. An independent accuracy indicator has been proposed by Cowan [14], i.e. the cancellation factor as defined below

$$CF = \left(\frac{\left|\sum\sum c'_k\left\langle\Phi'_k\left(\gamma'_k\Pi' J' M'_J\right)\left|D^{(1)}\right|\Phi_i\left(\gamma_i \Pi J M_J\right)\right\rangle c_i\right|}{\sum\sum\left|c'_k\left\langle\Phi'_k\left(\gamma'_k\Pi' J' M'_J\right)\right|D^{(1)}\left|\Phi_i\left(\gamma_i \Pi J M_J\right)\right\rangle c_i\right|}\right)^2 \tag{5}$$

where $D^{(1)}$ is the electric dipole operator and $c_{i(k)}(')$ and $\Phi_{i(k)}(')$ have the same meaning as in Eq. (1) for the initial (non-primed symbols) and final (primed symbols) states of the transition. A small value of the cancellation factor, e.g. less than 0.05, indicates that the computed line strength is affected by strong cancellation effects due to opposite sign contributions of almost equal and significant amplitudes that cancel each other in the transition amplitude expansions which are directly related to the ASF representation. The GRASP2K package has been modified such as to implement the calculation of this latter accuracy indicator (see our previous work on the Te II and Te III spectra [15] for a detailed discussion).

2.2. Semi-empirical HFR method

The Hartree–Fock with relativistic corrections (HFR) method of Cowan [14] has been considered as a second independent approach for computing the atomic structure and the transition rates in Xe XI. The configuration interaction (CI) expansions to represent the atomic state functions were $4d^8 + 4d^7 ns$ $(n = 5-7) + 4d^7 nd$

Table 1
Radial parameters (in cm^{-1}) adopted in the HFR calculations.

Configuration	Parameter	*Ab initio*	Fitted	Ratio
$4d^8$	E_{av}	0	27 125	/
	$F^2(4d,4d)$	124 483	107 804	0.866
	$F^4(4d,4d)$	83 642	76 474	0.914
	ζ_{4d}	6 757	6 906	1.022
$4d^7 5p$	E_{av}	739 288	761 204	/
	$F^2(4d,4d)$	126 191	109 570	0.868
	$F^4(4d,4d)$	84 905	75 420	0.888
	α	/	29	/
	T	/	−6	Fixed
	ζ_{4d}	6 976	7 244	1.038
	ζ_{5p}	16 240	17 321	1.067
	$F^2(4d,5p)$	50 524	45 348	0.898
	$G^1(4d,5p)$	14 855	12 823	0.863
	$G^3(4d,5p)$	14 920	13 661	0.916
$4d^7 4f$	E_{av}	745 883	766 888	/
	$F^2(4d,4d)$	124 965	103 286	0.827
	$F^4(4d,4d)$	83 991	69 502	0.828
	α	/	57	/
	T	/	−5	Fixed
	ζ_{4d}	6 830	7 003	1.025
	ζ_{4f}	512	651	1.272
	$F^2(4d,4f)$	109 020	104 488	0.958
	$F^4(4d,4f)$	70 559	59 377	0.841
	$G^1(4d,4f)$	130 235	110 477	0.848
	$G^3(4d,4f)$	82 220	69 251	0.842
	$G^5(4d,4f)$	58 296	47 593	0.816
$4p^5 4d^9$	E_{av}	760 427	790 936	/
	ζ_{4p}	68 097	66 454	0.976
	ζ_{4d}	6 784	7 125	1.050
	$F^2(4p,4d)$	130 813	94 080	0.719
	$G^1(4p,4d)$	166 218	117 360	0.706
	$G^3(4p,4d)$	104 292	71 480	0.685
$4d^7 5p - 4d^7 4f$	$R^2(4d,5p;4d,4f)$	−9 520	−7 555	0.794
	$R^4(4d,5p;4d,4f)$	−2326	−1 846	0.794
	$R^1(4d,5p;4f,4d)$	−2 606	−2 067	0.794
	$R^3(4d,5p;4f,4d)$	244	194	0.794
$4d^7 5p - 4p^5 4d^9$	$R^1(4p,5p;4d,4d)$	4 940	6 552	1.326
	$R^3(4p,5p;4d,4d)$	7 488	9 931	1.326
$4d^7 4f - 4p^5 4d^9$	$R^1(4p,4f;4d,4d)$	143 913	109 231	0.759
	$R^3(4p,4f;4d,4d)$	89 787	68 148	0.759

$(n=5-6)+4d^6 5s^2+4d^6 5p^2+4d^6 5d^2+4d^6 5s6s+4d^6 5s5d+4p^5 4d^8 5p$ in the even parity and $4d^7 np$ $(n=5-7)+4d^7 nf$ $(n=4-6)+4d^6 5snp$ $(n=5-6)+4d^6 5p5d+4p^5 4d^9$ in the odd parity. The interaction between these configurations is expected to include most of the valence and part of the core – valence electron correlation by the superposition of two configurations having one hole in the 4p core sub-shell (one in each parity).

Aiming at taking into account the effects of missing configurations and improving the mixing coefficients in the CI expansions, some hamiltonian radial parameters have been fitted so as to minimize the differences between the hamiltonian eigenvalues and all the experimental energy levels of Churilov et al. [7] in separate least-squares fit procedures, one for each parity. They corresponded to the average energies (E_{av}), monoconfiguration Slater integrals (F^k, G^k) and spin-orbit integrals (ζ) of the spectroscopic configurations, i.e. $4d^8$, $4d^7 5p$, $4d^7 4f$ and $4p^5 4d^9$, and CI Slater integrals (R^k) between them. During the fit of the odd parity, the effective interaction parameters α and T of the spectroscopic configurations $4d^7 5p$ and $4d^7 4f$ have also been considered : the formers have been fitted while the latters, expected to be small, being fixed to the values published by Churilov et al. [7]. The parameter values adopted in the final HFR calculation of the transition rates are reported in Table 1. All the other Slater integrals have been scaled down by a factor of 0.9, as suggested by Cowan [14] for moderately ionized atoms, while the spin-orbit integrals have been used unscaled. The average deviations of the fitting procedures were 167 cm^{-1} when considering all the nine levels of the even-parity ground configuration $4d^8$, and 192 cm^{-1} when minimizing the differences from 123 experimental levels belonging to the odd-parity configurations $(4p^5 4d^9+4d^7 5p+4d^7 4f)$.

The semi-empirical HFR transition probabilities and oscillator strengths have been determined in the length gauge using the fitted radial parameters given in Table 1 and their corresponding cancellation factors (see Eq. (5)) [14] have been estimated for all the electric dipole transitions between the ground configuration $4d^8$ and the first three excited odd configurations $4p^5 4d^9$, $4d^7 5p$ and $4d^7 4f$.

3. Results and discussions

In Table 2, we compare the calculated level energies obtained using our *ab initio* RCI-CV(4p) and semi-empirical HFR models with all the experimental values of Churilov et al. [7]. The matching of our RCI-CV(4p) levels with those of the other two models is done by tacking into account the level ordering within a given J-Π symmetry matrix block and the major non-relativistic electronic configuration compositions. The average deviation of our RCI-CV(4p) levels with experiment [7] is 2656 cm^{-1}. This represents less than 0.3% of the investigated energy range which is rather satisfactory for an *ab initio* model of a complex atomic structure such as Xe XI. The LS compositions as computed with our HFR model are also given. They are similar to those published by Churilov et al. [7]. In particular, the odd-parity states are strongly mixed showing a majority of leading components with purities of the order of 25% or less. This can cause destructive interferences in the computation of the line strengths which are measured through the cancellation factor (CF). Not shown in the table are the jj compositions as determined by our fully relativistic RCI-CV(4p) model. Those present also a large number of highly mixed states with potential consequence on the calculated transition rates, i.e. low CF values ($<$ 0.05).

The oscillator strengths together with the corresponding transition probabilities as computed by our two models (RCI-CV(4p) and HFR) are reported in Table 3 for all the electric dipole transitions between all the Xe XI levels given in Table 2. This represents 576 lines covering the EUV spectral range 102 Å–157 Å. For each transition, the CF value as estimated the LS coupling representation using the HFR method and in the jj coupling representation given by the RCI method along with the corresponding ratio (B/C) between the line strengths calculated in the Babushkin and the Coulomb gauges are also shown. The vast majority of the lines (about 85%) are affected by strong cancellation effects (with CF $<$ 0.05) in one or both of our models as the consequence of the strong mixing of the odd parity states, or/and their RCI line strengths have significant desagreements between the gauges (with B/C $<$ 0.9 or $>$ 1.1). Only transition rates having both CF $>$ 0.05 and 0.9 $<$ B/C $<$ 1.1 can be considered as fully reliable [15].

In Fig. 1, log gf values as computed with RCI-CV(4p) are compared with those obtained with HFR. We have excluded the transitions with CF $<$ 0.05 and with B/C $<$ 0.9 or $>$ 1.1 from the figure. We notice that, for the strongest lines (log gf $>$ 0), RCI-CV(4p) values are systematically about 20% smaller than the HFR results. Actually, the average ratio <gf(RCI-CV(4p)/gf(HFR)> is equal to 0.78 ± 0.19 (the second number being the standard deviation) for these transitions, i.e. a 20% systematic decrease. This is mainly due to the missing core – core and core – valence correlations related to missing configurations with more than one hole in the 4p core subshell in our HFR CI expansions. In constrast, those correlations were taken into account in our RCI calculations.

The CI effects of opening further the $n=4$ core shell can be appreciated from the comparison between our models RCI-CV(4p) and RCI-CV(4s,4p) as presented in Fig. 2.

Table 2
Comparison between our HFR, RCI-CV(4p) and the available experimental energy levels in Xe XI. The corresponding HFR *LS*-coupling compositions are also shown.

i	E_{Expt}[a] (cm^{-1})	E_{HFR} (cm^{-1})	E_{RCI} (cm^{-1})	*J*	*LS*-Coupling Composition[b] (%)
1	0	0	0	4	97 4d^8 ^{3}F + 3 4d^8 ^{1}G
2	13,140	13,559	14,530	2	43 4d^8 ^{1}D + 35 4d^8 ^{3}F + 21 4d^8 ^{3}P
3	15,205	15,016	15,073	3	100 4d^8 ^{3}F
4	26,670	26,707	27,923	2	55 4d^8 ^{3}P + 44 4d^8 ^{3}F
5	32,210	32,475	20,894	0	90 4d^8 ^{3}P + 10 4d^8 ^{1}S
6	34,610	34,734	37,076	1	100 4d^8 ^{3}P
7	40,835	40,699	43,491	4	97 4d^8 ^{1}G
8	42,900	43,196	44,648	2	56 4d^8 ^{1}D + 24 4d^8 ^{3}P + 20 4d^8 ^{3}F
9	88,130	88,285	78,939	0	90 4d^8 ^{1}S + 10 4d^8 ^{3}P
10	679,572	679,615	663,942	3	49 4p^{5}4d^9 (^{2}P)^{3}D + 19 4d^{7}4f (^{2}G)^{3}D + 13 4d^{7}4f (^{2}H)^{3}D
11	681,023	681,244	663,859	2	44 4p^{5}4d^9 (^{2}P)^{1}D + 16 4p^{5}4d^9 (^{2}P)^{3}P + 10 4d^{7}4f (^{2}G)^{1}D
12	687,020	686,940	670,382	4	64 4p^{5}4d^9 (^{2}P)^{3}F + 10 4d^{7}4f (^{2}H)^{3}F + 5 4d^{7}4f (^{2}P)^{3}F
13	695,376	695,734	693,085	4	44 4d^{7}5p (^{4}F)^{5}D + 24 4d^{7}5p (^{4}F)^{5}F + 12 4d^{7}5p (^{4}F)^{3}F
14	709,285	709,277	706,453	3	41 4d^{7}5p (^{4}F)^{5}F + 34 4d^{7}5p (^{4}F)^{5}D + 6 4d^{7}5p (^{4}P)^{5}D
15	712,223	712,604	710,419	4	45 4d^{7}5p (^{4}F)^{5}G + 18 4d^{7}5p (^{4}F)^{3}G + 15 4d^{7}5p (^{4}F)^{5}F
16	714,855	715,030	713,341	3	33 4d^{7}5p (^{4}F)^{5}G + 8 4d^{7}5p (^{4}F)^{3}F + 7 4d^{7}5p (^{4}P)^{5}D
17	715,730	716,068	717,676	2	15 4d^{7}5p (^{2}P)^{3}D + 10 4d^{7}5p (^{2}P)^{1}D + 10 4d^{7}5p (^{4}P)^{5}D
18	717,330	717,892	704,244	3	22 4p^{5}4d^9 (^{2}P)^{3}F + 13 4d^{7}4f (^{4}P)^{5}D + 12 4d^{7}4f (^{2}H)^{1}F
19	721,001	721,465	718,010	2	23 4d^{7}5p (^{4}F)^{5}G + 20 4d^{7}5p (^{4}P)^{5}D + 12 4d^{7}5p (^{4}F)^{5}D
20	722,439	722,311	719,623	5	54 4d^{7}5p (^{4}F)^{5}F + 25 4d^{7}5p (^{4}F)^{3}G + 6 4d^{7}5p (^{2}G)^{1}H
21	725,053	725,478	723,053	4	27 4d^{7}5p (^{4}F)^{5}D + 15 4d^{7}5p (^{4}F)^{3}F
22	725,825	726,057	724,796	3	18 4d^{7}5p (^{4}P)^{5}D + 18 4d^{7}5p (^{4}F)^{5}G + 15 4d^{7}5p (^{4}F)^{3}D
23	730,235	730,374	727,827	4	59 4d^{7}4f (^{4}F)^{5}I + 8 4d^{7}4f (^{2}G)^{3}H + 8 4d^{7}4f (^{2}D)^{3}H
24	730,345	730,709	729,767	5	19 4d^{7}5p (^{2}G)^{3}H + 16 4d^{7}5p (^{2}H)^{3}I + 13 4d^{7}5p (^{2}G)^{3}G
25	731,458	731,762	730,168	4	17 4d^{7}5p (^{4}F)^{3}F + 27 4d^{7}5p (^{4}F)^{5}F + 21 4d^{7}5p (^{2}G)^{3}F
26	733,755	734,164	732,592	3	37 4d^{7}5p (^{4}F)^{3}D + 11 4d^{7}5p (^{2}G)^{3}F + 10 4d^{7}5p (^{4}F)^{3}F
27	735,246	735,523	733,684	4	39 4d^{7}4f (^{4}P)^{5}G + 13 4d^{7}4f (^{4}F)^{5}G + 8 4d^{7}4f (^{2}P)^{3}G
28	736,077	735,952	737,053	5	30 4d^{7}4f (^{4}F)^{3}H + 21 4d^{7}4f (^{4}P)^{5}G + 9 4d^{7}4f (^{4}F)^{5}G
29	737,388	737,385	735,427	4	26 4d^{7}5p (^{4}F)^{5}F + 28 4d^{7}5p (^{4}F)^{3}F + 15 4d^{7}5p (^{4}F)^{3}G
30	738,248	738,151	735,085	5	51 4d^{7}5p (^{4}F)^{5}G + 16 4d^{7}5p (^{4}F)^{3}G + 14 4d^{7}5p (^{2}H)^{3}G
31	739,322	739,132	738,288	3	14 4d^{7}5p (^{4}F)^{5}D + 12 4d^{7}5p (^{4}F)^{5}F + 9 4d^{7}5p (^{4}P)^{3}D
32	739,542	739,692	738,939	4	57 4d^{7}5p (^{2}G)^{3}H + 8 4d^{7}5p (^{2}G)^{1}G + 5 4d^{7}5p (^{2}G)^{3}G
33	740,348	740,229	739,769	5	59 4d^{7}5p (^{2}H)^{3}G + 10 4d^{7}5p (^{4}F)^{3}G + 8 4d^{7}5p (^{4}F)^{5}G
34	740,757	740,918	745,743	2	24 4d^{7}5p (^{4}F)^{5}F + 13 4d^{7}5p (^{4}F)^{3}F + 8 4d^{7}5p (^{2}P)^{1}D
35	741,800	741,829	741,062	3	18 4d^{7}5p (^{2}G)^{3}G + 18 4d^{7}5p (^{2}G)^{1}F
36	742,430	742,664	742,294	5	25 4d^{7}4f (^{4}F)^{3}I + 16 4d^{7}4f (^{4}P)^{5}G + 15 4d^{7}4f (^{2}P)^{3}G
37	742,594	742,667	743,141	1	35 4d^{7}5p (^{2}P)^{3}D + 20 4d^{7}5p (^{4}F)^{5}D + 9 4d^{7}5p (^{2}D)^{3}D
38	744,537	744,594	741,434	4	41 4d^{7}5p (^{4}F)^{3}G + 22 4d^{7}5p (^{4}F)^{5}G + 10 4d^{7}5p (^{2}D)^{3}F
39	744,955	744,877	749,599	3	11 4d^{7}5p (^{2}D)^{3}D + 15 4d^{7}5p (^{4}F)^{3}F + 14 4d^{7}5p (^{4}F)^{5}G
40	745,470	745,497	744,771	1	23 4d^{7}5p (^{4}F)^{5}F + 14 4d^{7}5p (^{4}P)^{3}S + 5 4d^{7}5p (^{2}D)^{1}P
41	745,762	745,791	751,110	3	17 4d^{7}4f (^{2}G)^{1}F + 18 4d^{7}4f (^{2}G)^{3}F + 12 4d^{7}4f (^{4}F)^{3}F
42	746,445	746,300	752,542	3	22 4d^{7}5p (^{4}F)^{3}G + 12 4d^{7}5p (^{2}D)^{3}F + 12 4d^{7}5p (^{2}F)^{3}G
43	746,552	746,678	750,469	2	17 4d^{7}5p (^{4}F)^{3}F + 16 4d^{7}5p (^{4}F)^{5}F + 9 4d^{7}5p (^{2}D)^{3}F
44	748,644	748,514	745,579	1	22 4d^{7}4f (^{4}F)^{3}P + 14 4d^{7}4f (^{2}G)^{3}D + 10 4d^{7}4f (^{2}G)^{3}P
45	749,351	749,329	754,145	3	23 4d^{7}5p (^{4}F)^{3}F + 9 4d^{7}5p (^{2}D)^{3}F + 8 4d^{7}5p (^{2}F)^{3}G
46	750,512	750,654	753,965	2	42 4d^{7}5p (^{4}F)^{3}D + 10 4d^{7}5p (^{2}P)^{3}P + 10 4d^{7}5p (^{2}G)^{3}F
47	752,054	752,057	759,117	3	13 4d^{7}5p (^{2}G)^{1}F + 9 4d^{7}5p (^{2}P)^{3}D + 9 4d^{7}5p (^{2}D)^{3}D
48	752,155	752,320	751,715	1	27 4d^{7}5p (^{4}F)^{5}D + 24 4d^{7}5p (^{4}F)^{3}D + 14 4d^{7}5p (^{4}P)^{5}D
49	752,285	752,779	743,279	4	58 4d^{7}5p (^{4}P)^{5}D + 10 4d^{7}5p (^{2}G)^{3}F + 5 4d^{7}5p (^{4}F)^{3}G
50	753,352	753,656	753,820	5	61 4d^{7}5p (^{2}H)^{3}I + 22 4d^{7}5p (^{2}G)^{3}G + 7 4d^{7}5p (^{2}G)^{3}H
51	753,795	753,812	756,577	2	20 4d^{7}5p (^{4}F)^{3}D + 14 4d^{7}5p (^{4}P)^{5}P + 11 4d^{7}5p (^{4}F)^{3}F
52	754,745	755,105	756,170	1	35 4d^{7}5p (^{2}P)^{1}P + 14 4d^{7}5p (^{2}P)^{3}D + 11 4d^{7}5p (^{4}P)^{5}P
53	754,860	754,831	761,515	3	37 4d^{7}5p (^{4}F)^{3}G + 10 4d^{7}5p (^{2}P)^{3}D + 8 4d^{7}5p (^{2}F)^{3}G
54	755,831	755,772	754,482	4	15 4d^{7}5p (^{2}G)^{3}F + 12 4d^{7}5p (^{2}G)^{1}G + 9 4d^{7}4f (^{2}G)^{3}H
55	756,016	755,951	756,246	4	46 4d^{7}5p (^{2}H)^{3}G + 11 4d^{7}5p (^{2}F)^{3}G + 10 4d^{7}5p (^{2}G)^{3}G
56	756,170	756,187	759,784	2	21 4d^{7}5p (^{4}P)^{3}D + 18 4d^{7}5p (^{2}D)^{3}P + 11 4d^{7}5p (^{2}F)^{1}D
57	758,337	758,494	759,792	1	23 4d^{7}5p (^{4}P)^{3}S + 19 4d^{7}5p (^{4}F)^{3}D + 10 4d^{7}5p (^{2}P)^{3}D
58	759,110	759,451	767,624	3	26 4d^{7}5p (^{4}P)^{5}P + 15 4d^{7}5p (^{4}P)^{3}D + 11 4d^{7}5p (^{2}G)^{3}F
59	759,260	759,463	758,723	5	32 4d^{7}5p (^{2}G)^{3}G + 26 4d^{7}5p (^{2}G)^{1}H + 15 4d^{7}5p (^{2}H)^{3}H
60	760,950	760,932	767,222	1	22 4d^{7}5p (^{4}P)^{3}S + 15 4d^{7}5p (^{4}P)^{3}P
61	761,266	761,337	769,361	3	26 4d^{7}5p (^{2}G)^{3}G + 18 4d^{7}5p (^{4}P)^{3}D + 10 4d^{7}5p (^{4}P)^{5}P
62	762,105	762,093	762,797	2	21 4d^{7}5p (^{2}D)^{3}F + 19 4d^{7}5p (^{2}G)^{3}F + 8 4d^{7}5p (^{2}P)^{3}P
63	763,070	763,376	763,633	4	31 4d^{7}5p (^{2}G)^{3}G + 18 4d^{7}5p (^{2}G)^{3}H + 14 4d^{7}5p (^{2}H)^{1}H
64	765,052	764,898	764,887	2	31 4d^{7}5p (^{4}P)^{3}P + 18 4d^{7}5p (^{2}P)^{3}D + 13 4d^{7}5p (^{4}P)^{5}P
65	765,770	765,969	769,546	1	34 4d^{7}5p (^{4}P)^{3}P + 21 4d^{7}5p (^{2}P)^{3}P + 17 4d^{7}5p (^{2}P)^{3}P
66	766,625	767,010	768,210	2	15 4d^{7}5p (^{2}G)^{3}F + 8 4d^{7}4f (^{2}P)^{3}F + 7 4d^{7}4f (^{2}F)^{3}F
67	766,860	766,864	775,081	3	28 4d^{7}5p (^{2}G)^{3}G + 19 4d^{7}5p (^{2}F)^{3}D + 8 4d^{7}5p (^{4}P)^{5}P
68	766,947	766,976	767,117	5	24 4d^{7}5p (^{2}G)^{3}H + 19 4d^{7}5p (^{2}G)^{1}H + 11 4d^{7}4f (^{4}P)^{5}F
69	767,369	767,526	767,705	1	27 4d^{7}5p (^{2}D)^{3}D + 24 4d^{7}5p (^{4}P)^{3}D + 8 4d^{7}5p (^{2}P)^{3}S
70	767,700	768,074	769,415	5	17 4d^{7}5p (^{2}G)^{3}H + 16 4d^{7}5p (^{2}G)^{1}H + 9 4d^{7}4f (^{4}P)^{3}G
71	768,773	768,997	776,607	3	21 4d^{7}5p (^{4}P)^{5}D + 12 4d^{7}5p (^{2}P)^{3}D + 12 4d^{7}5p (^{2}F)^{3}D
72	769,217	769,500	772,076	2	21 4d^{7}4f (^{4}P)^{5}F + 8 4p^{5}4d^9 (^{2}P)^{3}P + 6 4d^{7}4f (^{2}D)^{3}P

(*continued on next page*)

Table 2 (*continued*)

i	E_{Expt}[a] (cm^{-1})	E_{HFR} (cm^{-1})	E_{RCI} (cm^{-1})	J	*LS*-Coupling Composition[b] (%)
73	772,875	773,057	776,265	4	15 $4d^75p\,(^2D)^3F$ + 11 $4d^74f\,(^2D)^1G$ + 6 $4d^75p\,(^2F)^1G$
74	773,315	773,861	777,687	2	14 $4d^75p\,(^2P)^3D$ + 13 $4d^75p\,(^4F)^3F$ + 9 $4d^75p\,(^2D)^1D$
75	773,363	773,494	781,961	4	27 $4d^74f\,(^4P)^5F$ + 10 $4d^74f\,(^2D)^3G$ + 7 $4d^75p\,(^2G)^1G$
76	773,519	773,591	778,326	5	16 $4d^74f\,(^2H)^1H$ + 13 $4d^75p\,(^2H)^3H$ + 4 $4d^74f\,(^2D)^1H$
77	773,715	773,556	782,032	3	29 $4d^75p\,(^2G)^1F$ + 23 $4d^75p\,(^2G)^3G$ + 15 $4d^75p\,(^2F)^3G$
78	773,968	774,200	776,764	4	17 $4d^75p\,(^2G)^1G$ + 15 $4d^75p\,(^2H)^1G$ + 9 $4d^74f\,(^4P)^5F$
79	773,968	774,159	773,930	5	29 $4d^75p\,(^2H)^3H$ + 20 $4d^75p\,(^2H)^1H$ + 9 $4d^75p\,(^2H)^3G$
80	775,030	775,156	776,693	1	26 $4d^75p\,(^2D)^3P$ + 11 $4d^75p\,(^2D)^1P$ + 10 $4d^75p\,(^2P)^1P$
81	775,570	775,670	782,939	3	14 $4d^75p\,(^2H)^3G$ + 14 $4d^75p\,(^2D)^1F$ + 13 $4d^75p\,(^2F)^3F$
82	775,775	776,170	772,343	4	16 $4d^75p\,(^2H)^1G$ + 17 $4d^75p\,(^2D)^3F$ + 12 $4d^75p\,(^2F)^3G$
83	776,253	776,287	792,231	3	17 $4d^74f\,(^4P)^3F$ + 16 $4d^74f\,(^2F)^3F$ + 7 $4d^75p\,(^2H)^3G$
84	776,787	776,939	786,262	4	36 $4d^74f\,(^4P)^3F$ + 12 $4d^74f\,(^2H)^3H$ + 8 $4d^74f\,(^2D)^3H$
85	778,350	778,537	779,079	1	28 $4d^75p\,(^4P)^3D$ + 21 $4d^75p\,(^2D)^1P$ + 10 $4d^75p\,(^2D)^3P$
86	780,503	780,909	790,070	3	15 $4d^75p\,(^2H)^3G$ + 8 $4d^75p\,(^2D)^1F$ + 2 $4d^74f\,(^2F)^3G$
87	780,805	781,375	778,266	2	13 $4d^74f\,(^4F)^3P$ + 9 $4d^75p\,(^4P)^3P$ + 8 $4d^74f\,(^2D)^3P$
88	781,822	781,877	782,981	2	10 $4d^75p\,(^2D)^3P$ + 8 $4d^75p\,(^2D)^3D$ + 8 $4d^75p\,(^2P)^1D$
89	784,035	784,295	786,240	1	23 $4d^75p\,(^2P)^3S$ + 23 $4d^75p\,(^2D)^1P$ + 10 $4d^75p\,(^2P)^3P$
90	784,826	784,722	794,106	3	32 $4d^74f\,(^2F)^3G$ + 13 $4d^74f\,(^2H)^3G$ + 7 $4d^74f\,(^2F)^3F$
91	786,580	786,584	786,284	2	12 $4d^75p\,(^2F)^3D$ + 11 $4d^75p\,(^2D)^1D$ + 9 $4d^75p\,(^2P)^3P$
92	787,403	787,663	801,000	1	27 $4d^74f\,(^2F)^3P$ + 19 $4d^74f\,(^2D)^3P$ + 16 $4d^74f\,(^2D)^3P$
93	788,145	788,263	790,003	2	15 $4d^75p\,(^2P)^1D$ + 14 $4d^75p\,(^2F)^3D$ + 13 $4d^75p\,(^2F)^3F$
94	788,396	788,559	760,425	1	46 $4d^75p\,(^2F)^3D$ + 10 $4d^74f\,(^2F)^3P$ + 9 $4d^75p\,(^2D)^3D$
95	788,465	788,896	797,265	3	18 $4d^75p\,(^2F)^3F$ + 13 $4d^74f\,(^4P)^3F$ + 7 $4d^75p\,(^2F)^3G$
96	789,029	789,355	790,226	5	48 $4d^75p\,(^2H)^1H$ + 16 $4d^75p\,(^2H)^3H$ + 8 $4d^75p\,(^2H)^3I$
97	791,395	791,338	801,644	3	14 $4d^74f\,(^2F)^3D$ + 13 $4d^74f\,(^2F)^3G$ + 11 $4d^74f\,(^2D)^3D$
98	791,805	791,824	812,006	1	21 $4d^75p\,(^2D)^3P$ + 20 $4d^75p\,(^2D)^1P$ + 10 $4d^75p\,(^2D)^3D$
99	792,311	792,702	822,427	0	63 $4d^75p\,(^2D)^3P$ + 11 $4d^75p\,(^2P)^1S$ + 6 $4d^75p\,(^2P)^3P$
100	794,365	794,711	790,696	2	30 $4d^74f\,(^2D)^3P$ + 21 $4d^74f\,(^2F)^3P$ + 7 $4d^75p\,(^2F)^3D$
101	795,135	795,089	805,101	3	24 $4d^75p\,(^2D)^1F$ + 16 $4d^75p\,(^2P)^3D$ + 15 $4d^75p\,(^2F)^1F$
102	795,995	796,012	797,570	2	18 $4d^75p\,(^2F)^1D$ + 14 $4d^75p\,(^2F)^3D$ + 12 $4d^74f\,(^2D)^3P$
103	801,225	801,399	812,940	3	41 $4d^75p\,(^2F)^1F$ + 14 $4d^75p\,(^2D)^3F$ + 10 $4d^75p\,(^2D)^3F$
104	802,905	802,647	804,979	2	39 $4d^75p\,(^2D)^3P$ + 18 $4d^75p\,(^2F)^1D$ + 8 $4d^75p\,(^2D)^3P$
105	808,130	808,021	826,366	1	31 $4d^75p\,(^2D)^3P$ + 14 $4d^75p\,(^2D)^3D$ + 13 $4d^75p\,(^2D)^3D$
106	824,474	824,671	827,985	3	43 $4d^75p\,(^2D)^1F$ + 30 $4d^75p\,(^2D)^3F$ + 6 $4d^75p\,(^2D)^3D$
107	828,875	828,799	833,419	2	57 $4d^75p\,(^2D)^3D$ + 10 $4d^75p\,(^2D)^3D$ + 10 $4d^75p\,(^2D)^1D$
108	830,260	830,943	834,618	1	47 $4d^75p\,(^2D)^1P$ + 32 $4d^75p\,(^2D)^3D$ + 5 $4d^75p\,(^2D)^1P$
109	838,289	838,480	843,673	3	50 $4d^75p\,(^2D)^3D$ + 20 $4d^75p\,(^2D)^3D$ + 9 $4d^75p\,(^2D)^1F$
110	892,420	892,825	911,549	4	36 $4d^74f\,(^4F)^3F$ + 19 $4d^74f\,(^2H)^3F$ + 17 $4d^74f\,(2G)^3F$
111	894,941	895,389	915,612	3	29 $4d^74f\,(^2H)^3D$ + 18 $4p^54d^9\,(^2P)^3D$ + 16 $4d^74f\,(^4F)^3D$
112	897,383	897,112	913,317	5	40 $4d^74f\,(^4F)^3G$ + 17 $4d^74f\,(^4P)^3G$ + 11 $4d^74f\,(^2G)^3G$
113	902,577	902,747	926,707	1	27 $4d^74f\,(2G)^1P$ + 14 $4d^74f\,(^2F)^3S$ + 13 $4d^74f\,(^4F)^3S$
114	907,711	908,021	927,213	2	13 $4d^74f\,(2G)^1D$ + 12 $4d^74f\,(^4F)^3F$ + 7 $4d^74f\,(^2H)^3F$
115	908,390	908,255	927,233	3	13 $4d^74f\,(^2P)^1F$ + 12 $4d^74f\,(^2D)^1F$
116	911,082	911,390	927,829	4	39 $4d^74f\,(^4F)^3G$ + 16 $4d^74f\,(^4P)^3G$ + 11 $4d^74f\,(^2D)^3G$
117	911,665	911,766	931,204	2	19 $4d^74f\,(^2H)^3D$ + 15 $4p^54d^9\,(^2P)^3D$ + 11 $4d^74f\,(^4F)^3D$
118	912,600	912,902	931,405	3	17 $4d^74f\,(^4F)^3F$ + 10 $4d^74f\,(^4F)^3G$ + 9 $4d^74f\,(^2H)^3F$
119	913,877	913,950	937,241	1	31 $4d^74f\,(^2F)^3S$ + 31 $4d^74f\,(^4F)^3S$ + 7 $4d^74f\,(^2H)^3D$
120	922,295	922,378	940,551	3	22 $4d^74f\,(^4P)^3D$ + 13 $4d^74f\,(^4F)^3G$ + 8 $4d^74f\,(^2D)^3D$
121	924,500	924,529	944,167	2	23 $4d^74f\,(^4P)^3D$ + 10 $4d^74f\,(^4F)^3F$ + 9 $4d^74f\,(^2D)^3D$
122	925,010	925,340	946,700	1	13 $4d^74f\,(^2F)^3P$ + 13 $4d^74f\,(^4F)^3P$
123	925,626	925,731	949,024	4	51 $4d^74f\,(^2H)^1G$ + 21 $4d^74f\,(^2G)^1G$ + 15 $4d^74f\,(^2F)^1G$
124	931,420	931,397	951,049	1	21 $4d^74f\,(^4P)^3D$ + 11 $4d^74f\,(^2F)^3P$ + 4 $4d^74f\,(^2D)^3P$
125	933,343	933,305	953,039	0	30 $4d^74f\,(^2F)^3P$ + 27 $4d^74f\,(^4F)^3P$ + 21 $4p^54d^9\,(^2P)^3P$
126	935,035	935,276	954,778	3	17 $4d^74f\,(^2P)^1F$ + 15 $4d^74f\,(^2D)^1F$ + 12 $4d^74f\,(^4F)^3G$
127	938,628	938,984	957,904	5	27 $4d^74f\,(^2F)^1H$ + 26 $4d^74f\,(^2H)^1H$ + 18 $4d^74f\,(^2G)^1H$
128	944,705	944,713	962,715	2	16 $4p^54d^9\,(^2P)^3D$ + 11 $4p^54d^9\,(^2P)^3F$ + 6 $4d^74f\,(^2G)^1D$
129	947,660	947,765	971,088	1	37 $4d^74f\,(^2D)^1P$ + 16 $4p^54d^9\,(^2P)^3D$ + 10 $4d^74f\,(^2G)^1P$
130	951,795	952,053	970,729	2	21 $4p^54d^9\,(^2P)^3P$ + 15 $4d^74f\,(^2F)^3P$ + 12 $4d^74f\,(^4F)^3P$
131	957,488	957,574	980,338	3	41 $4p^54d^9\,(^2P)^1F$ + 24 $4d^74f\,(^2H)^1F$ + 8 $4p^54d^9\,(^2P)^3D$
132	989,020	989,093	1,015,994	1	45 $4d^74f\,(^2D)^1P$ + 21 $4p^54d^9\,(^2P)^1P$

[a] Experimental energy level values taken from [7].

[b] HFR composition in *LS*-coupling. Only the first three components greater or equal to 5% are given.

Here again, transitions with CF>0.05 and $0.9 < B/C < 1.1$ have been exclusively retained.

From this figure, one can see that these CI do not generate further systematics on the oscillator strengths; the average ratio <gf(RCI-CV(4 s,4p))/gf(RCI-CV(4p))> being 0.98 ± 0.12 for the strongest lines, i.e. log gf>0. We are therefore confident that our RCI-CV(4p) model takes into account the main core-excitation CI effects. This also implies that the major correlation effects within the $n = 4$ shell on the oscillator strengths have been considered in our RCI-CV(4p) model.

As expected for a highly charged ion such as Xe XI, the correlation with orbitals outside the Layzer complex has very small effects on the oscillator strengths as shown in Fig. 3 where our RCI-V(5f) model is compared to our RCI-V(6f) model. The average

Table 3
HFR and RCI-CV(4p) oscillator strengths (log gf) and transition probabilities (gA) in Xe XI.

λ (Å)[a]	Lower Level[b]			Upper Level[b]			HFR			RCI-CV(4p)			
	i	E (cm^{-1})	J	i	E (cm^{-1})	J	log gf	gA (s^{-1})	CF[c]	log gf	gA (s^{-1})	CF[c]	B/C[d]
102.472	2	13,140	2	132	989,020	1	−1.89	8.15E+09	0.00	−2.65	1.48E+09	0.00	0.90
103.912	4	26,670	2	132	989,020	1	−0.65	1.39E+11	0.09	−0.74	1.20E+11	0.05	1.02
104.440	1	0	4	131	957,488	3	−0.55	1.74E+11	0.04	−0.76	1.12E+11	0.02	0.99
104.514	5	32,210	0	132	989,020	1	−0.71	1.20E+11	0.04	−1.12	4.98E+10	0.01	1.00
104.777	6	34,610	1	132	989,020	1	−2.79	9.84E+08	0.00	−3.77	1.10E+08	0.00	0.68
105.695	8	42,900	2	132	989,020	1	0.29	1.15E+12	0.47	0.12	8.33E+11	0.23	1.01
105.893	2	13,140	2	131	957,488	3	−0.76	1.04E+11	0.04	−0.60	1.55E+11	0.05	1.19
106.125	3	15,205	3	131	957,488	3	0.23	1.00E+12	0.94	0.06	7.20E+11	0.06	1.04
106.535	2	13,140	2	130	951,795	2	−1.93	6.89E+09	0.00	−1.77	1.03E+10	0.00	0.80
106.538	1	0	4	127	938,628	5	−2.47	2.01E+09	0.00	−2.94	6.97E+08	0.00	0.74
106.770	3	15,205	3	130	951,795	2	0.22	9.72E+11	0.91	0.14	8.35E+11	0.11	1.02
106.948	1	0	4	126	935,035	3	−2.00	5.87E+09	0.01	−4.83	8.92E+06	0.00	0.02
107.007	2	13,140	2	129	947,660	1	−0.49	1.88E+11	0.05	−0.96	6.73E+10	0.03	0.82
107.346	2	13,140	2	128	944,705	2	−0.40	2.31E+11	0.03	−0.36	2.62E+11	0.07	1.11
107.432	4	26,670	2	131	957,488	3	−0.11	4.45E+11	0.34	−0.44	2.20E+11	0.03	0.99
107.585	3	15,205	3	128	944,705	2	0.11	7.47E+11	0.17	−0.07	5.09E+11	0.16	0.95
108.035	1	0	4	123	925,626	4	−1.89	7.29E+09	0.00	−4.75	1.07E+07	0.00	0.04
108.094	4	26,670	2	130	951,795	2	0.22	9.54E+11	0.15	0.09	7.36E+11	0.07	1.01
108.425	1	0	4	120	922,295	3	−0.04	5.18E+11	0.17	−0.32	2.84E+11	0.07	0.85
108.472	2	13,140	2	126	935,035	3	−0.96	6.16E+10	0.00	−1.71	1.15E+10	0.00	1.03
108.579	4	26,670	2	129	947,660	1	−0.26	3.11E+11	0.12	−0.40	2.38E+11	0.06	1.05
108.716	3	15,205	3	126	935,035	3	−2.31	2.76E+09	0.00	−1.49	1.92E+10	0.00	1.30
108.899	2	13,140	2	124	931,420	1	−1.41	2.19E+10	0.01	−0.77	9.96E+10	0.04	0.95
108.928	4	26,670	2	128	944,705	2	0.44	1.57E+12	0.26	0.38	1.39E+12	0.15	1.05
109.029	6	34,610	1	130	951,795	2	0.74	3.05E+12	0.96	0.65	2.61E+12	0.43	1.02
109.093	7	40,835	4	131	957,488	3	1.28	1.07E+13	0.90	1.18	8.96E+12	0.46	1.02
109.236	5	32,210	0	129	947,660	1	0.11	7.21E+11	0.39	−0.11	4.71E+11	0.12	1.03
109.339	8	42,900	2	131	957,488	3	0.39	1.36E+12	0.46	0.30	1.17E+12	0.24	1.07
109.523	6	34,610	1	129	947,660	1	−4.32	2.65E+07	0.00	−2.37	2.47E+09	0.01	1.11
109.577	1	0	4	118	912,600	3	−0.40	2.24E+11	0.05	−0.45	2.06E+11	0.05	1.01
109.665	2	13,140	2	122	925,010	1	−0.29	2.86E+11	0.09	−0.41	2.24E+11	0.06	0.97
109.726	2	13,140	2	121	924,500	2	−1.86	7.58E+09	0.00	−1.77	9.85E+09	0.00	1.62
109.760	1	0	4	116	911,082	4	−0.58	1.46E+11	0.05	−0.84	8.27E+10	0.02	1.00
109.839	3	15,205	3	123	925,626	4	−0.76	9.71E+10	0.23	−1.19	3.76E+10	0.00	1.03
109.879	6	34,610	1	128	944,705	2	0.67	2.56E+12	0.97	0.55	2.03E+12	0.47	1.02
109.975	3	15,205	3	121	924,500	2	−0.18	3.61E+11	0.22	−0.84	8.37E+10	0.02	0.79
109.992	2	13,140	2	120	922,295	3	−3.29	2.86E+08	0.00	−2.02	5.50E+09	0.00	1.25
110.024	8	42,900	2	130	951,795	2	0.94	4.79E+12	0.62	0.84	3.92E+12	0.42	1.02
110.085	1	0	4	115	908,390	3	−0.09	4.49E+11	0.23	−0.43	2.12E+11	0.05	0.93
110.088	4	26,670	2	126	935,035	3	−0.29	2.85E+11	0.04	−0.57	1.53E+11	0.01	1.01
110.243	3	15,205	3	120	922,295	3	−0.87	7.40E+10	0.03	−0.74	1.05E+11	0.01	0.99
110.527	8	42,900	2	129	947,660	1	0.74	2.99E+12	0.90	0.72	2.98E+12	0.47	1.11
110.528	4	26,670	2	124	931,420	1	0.45	1.53E+12	0.53	0.17	8.36E+11	0.15	0.97
110.889	8	42,900	2	128	944,705	2	0.91	4.38E+12	0.67	0.82	3.72E+12	0.28	1.03
111.001	9	88,130	0	132	989,020	1	0.92	4.50E+12	0.98	0.85	4.16E+12	0.60	1.08
111.020	2	13,140	2	119	913,877	1	−0.59	1.40E+11	0.04	−1.10	4.47E+10	0.01	0.98
111.178	2	13,140	2	118	912,600	3	0.56	1.97E+12	0.32	0.26	1.02E+12	0.19	1.03
111.209	5	32,210	0	124	931,420	1	−0.42	2.05E+11	0.05	0.11	7.37E+11	0.41	1.09
111.268	6	34,610	1	125	933,343	0	0.55	1.91E+12	0.98	0.45	1.58E+12	0.50	1.02
111.294	2	13,140	2	117	911,665	2	0.77	3.17E+12	0.65	0.35	1.27E+12	0.17	1.00
111.316	4	26,670	2	122	925,010	1	−0.06	4.75E+11	0.16	−0.12	4.26E+11	0.12	0.99
111.380	4	26,670	2	121	924,500	2	1.09	6.60E+12	0.85	0.98	5.39E+12	0.43	1.06
111.384	7	40,835	4	127	938,628	5	1.60	2.16E+13	0.98	1.51	1.82E+13	0.55	1.03
111.434	3	15,205	3	118	912,600	3	1.26	9.86E+12	0.98	1.20	8.97E+12	0.50	1.06
111.435	1	0	4	112	897,383	5	1.59	2.11E+13	0.98	1.51	1.79E+13	0.57	1.04
111.506	6	34,610	1	124	931,420	1	0.83	3.64E+12	0.98	0.71	2.86E+12	0.47	1.04
111.550	3	15,205	3	117	911,665	2	0.90	4.21E+12	0.90	0.94	4.90E+12	0.41	1.06
111.622	3	15,205	3	116	911,082	4	1.50	1.69E+13	0.98	1.42	1.45E+13	0.56	1.04
111.654	4	26,670	2	120	922,295	3	1.34	1.18E+13	0.96	1.27	1.03E+13	0.50	1.05
111.701	2	13,140	2	115	908,390	3	1.29	1.05E+13	0.96	1.25	9.78E+12	0.52	1.05
111.739	1	0	4	111	894,941	3	1.32	1.13E+13	0.94	1.25	9.84E+12	0.47	1.06
111.785	2	13,140	2	114	907,711	2	1.04	5.79E+12	0.66	1.05	6.18E+12	0.47	1.03
111.832	7	40,835	4	126	935,035	3	0.23	9.07E+11	0.50	0.16	7.94E+11	0.28	1.10
111.959	3	15,205	3	115	908,390	3	0.47	1.56E+12	0.29	0.15	7.88E+11	0.17	1.10
112.007	5	32,210	0	122	925,010	1	0.89	4.16E+12	0.96	0.77	3.37E+12	0.58	1.08
112.044	3	15,205	3	114	907,711	2	0.72	2.80E+12	0.87	0.38	1.33E+12	0.29	1.08
112.055	1	0	4	110	892,420	4	1.48	1.59E+13	0.98	1.39	1.37E+13	0.52	1.06
112.091	8	42,900	2	126	935,035	3	1.34	1.15E+13	0.94	1.25	9.94E+12	0.54	1.06
112.309	6	34,610	1	122	925,010	1	−0.72	1.01E+11	0.03	0.02	5.81E+11	0.34	1.04
112.373	6	34,610	1	121	924,500	2	0.60	2.09E+12	0.32	0.60	2.17E+12	0.29	1.08
112.431	2	13,140	2	113	902,577	1	0.94	4.61E+12	0.93	0.87	4.11E+12	0.48	1.09
112.547	8	42,900	2	124	931,420	1	−0.19	3.37E+11	0.17	−0.27	2.93E+11	0.10	1.11
112.713	4	26,670	2	119	913,877	1	0.73	2.81E+12	0.70	0.72	2.89E+12	0.38	1.10

(continued on next page)

Table 3 (*continued*)

λ (Å)[a]	Lower Level[b]			Upper Level[b]				HFR			RCI-CV(4p)		
	i	E (cm^{-1})	J	i	E (cm^{-1})	J	log gf	gA (s^{-1})	CF[c]	log gf	gA (s^{-1})	CF[c]	B/C[d]
112.876	4	26,670	2	118	912,600	3	−0.30	2.63E+11	0.06	−0.26	2.96E+11	0.03	1.09
112.995	4	26,670	2	117	911,665	2	−0.72	9.96E+10	0.03	−0.30	2.76E+11	0.03	0.93
113.021	7	40,835	4	123	925,626	4	1.46	1.49E+13	0.97	1.39	1.33E+13	0.54	1.11
113.365	8	42,900	2	122	925,010	1	−0.06	4.57E+11	0.15	−0.38	2.26E+11	0.12	1.23
113.404	2	13,140	2	111	894,941	3	−0.05	4.60E+11	0.20	−0.31	2.63E+11	0.06	1.15
113.415	4	26,670	2	115	908,390	3	−1.42	1.96E+10	0.00	−2.08	4.49E+09	0.00	1.13
113.422	5	32,210	0	119	913,877	1	−2.24	2.98E+09	0.00	−2.12	4.22E+09	0.02	0.79
113.430	8	42,900	2	121	924,500	2	−0.78	8.51E+10	0.03	−0.73	1.01E+11	0.01	0.97
113.448	7	40,835	4	120	922,295	3	0.17	7.72E+11	0.50	−0.09	4.34E+11	0.09	1.03
113.502	4	26,670	2	114	907,711	2	−2.66	1.13E+09	0.00	−1.33	2.55E+10	0.00	0.92
113.670	3	15,205	3	111	894,941	3	−0.60	1.29E+11	0.03	−0.42	2.07E+11	0.08	1.08
113.715	8	42,900	2	120	922,295	3	−1.11	4.01E+10	0.01	−1.29	2.72E+10	0.00	1.02
113.731	6	34,610	1	119	913,877	1	0.48	1.56E+12	0.57	0.33	1.15E+12	0.30	1.17
113.997	3	15,205	3	110	892,420	4	−0.70	1.02E+11	0.04	−1.00	5.36E+10	0.02	1.13
114.018	6	34,610	1	117	911,665	2	0.45	1.44E+12	0.51	0.32	1.11E+12	0.21	1.11
114.167	4	26,670	2	113	902,577	1	−0.75	9.03E+10	0.03	−0.99	5.54E+10	0.01	1.25
114.534	6	34,610	1	114	907,711	2	−0.32	2.47E+11	0.15	−1.05	4.75E+10	0.03	1.28
114.710	7	40,835	4	118	912,600	3	−0.01	4.93E+11	0.35	−0.12	3.98E+11	0.04	0.99
114.814	8	42,900	2	119	913,877	1	−0.11	3.91E+11	0.14	−0.24	3.06E+11	0.07	1.13
114.894	5	32,210	0	113	902,577	1	−0.22	3.07E+11	0.19	−0.26	3.04E+11	0.15	1.27
114.910	7	40,835	4	116	911,082	4	−0.83	7.44E+10	0.20	−1.21	3.19E+10	0.00	1.14
114.982	8	42,900	2	118	912,600	3	−0.80	7.96E+10	0.02	−1.55	1.49E+10	0.00	1.48
115.106	8	42,900	2	117	911,665	2	−1.68	1.06E+10	0.00	−5.07	4.47E+06	0.00	0.07
115.171	4	26,670	2	111	894,941	3	−0.20	3.14E+11	0.11	−0.46	1.83E+11	0.06	1.31
115.212	6	34,610	1	113	902,577	1	−1.31	2.48E+10	0.02	−2.68	1.11E+09	0.00	2.13
115.266	7	40,835	4	115	908,390	3	−0.22	3.05E+11	0.33	−0.31	2.57E+11	0.06	1.10
115.541	8	42,900	2	115	908,390	3	−2.35	2.22E+09	0.00	−2.85	7.42E+08	0.00	0.74
115.632	8	42,900	2	114	907,711	2	−0.83	7.35E+10	0.01	−0.82	7.90E+10	0.03	0.88
116.323	8	42,900	2	113	902,577	1	−2.15	3.48E+09	0.00	−3.92	6.21E+07	0.00	0.27
116.343	9	88,130	0	129	947,660	1	0.30	9.80E+11	0.38	0.18	8.01E+11	0.25	1.15
116.748	7	40,835	4	112	897,383	5	−2.97	5.23E+08	0.00	−4.07	4.26E+07	0.00	14.83
117.081	7	40,835	4	111	894,941	3	−1.14	3.50E+10	0.02	−1.30	2.54E+10	0.00	0.95
117.365	8	42,900	2	111	894,941	3	−1.48	1.59E+10	0.01	−1.82	7.62E+09	0.01	2.37
117.428	7	40,835	4	110	892,420	4	−2.98	5.02E+08	0.00	−2.92	5.99E+08	0.00	0.49
118.583	9	88,130	0	124	931,420	1	−3.22	2.83E+08	0.00	−3.56	1.41E+08	0.00	0.38
119.291	1	0	4	109	838,289	3	−1.26	2.55E+10	0.04	−1.27	2.53E+10	0.04	1.09
119.491	9	88,130	0	122	925,010	1	−1.74	8.59E+09	0.01	−1.67	1.08E+10	0.00	1.31
121.102	9	88,130	0	119	913,877	1	−3.16	3.11E+08	0.00	−2.21	3.06E+09	0.01	0.78
121.190	2	13,140	2	109	838,289	3	−2.28	2.40E+09	0.00	−2.69	9.45E+08	0.00	1.03
121.289	1	0	4	106	824,474	3	−2.22	2.72E+09	0.01	−2.19	2.93E+09	0.01	1.10
121.494	3	15,205	3	109	838,289	3	−2.39	1.86E+09	0.01	−2.20	2.90E+09	0.00	1.15
122.381	2	13,140	2	108	830,260	1	−2.19	2.90E+09	0.01	−2.11	3.45E+09	0.00	1.08
122.589	2	13,140	2	107	828,875	2	−2.02	4.23E+09	0.01	−2.75	8.01E+08	0.00	1.06
122.783	9	88,130	0	113	902,577	1	−2.85	6.18E+08	0.00	−3.75	8.62E+07	0.00	838.21
122.900	3	15,205	3	107	828,875	2	−1.18	2.95E+10	0.08	−1.34	2.03E+10	0.02	1.08
123.211	4	26,670	2	109	838,289	3	−1.64	1.00E+10	0.02	−1.47	1.51E+10	0.01	1.08
123.254	2	13,140	2	106	824,474	3	−3.36	1.90E+08	0.00	−3.29	2.27E+08	0.00	0.97
123.568	3	15,205	3	106	824,474	3	−2.29	2.25E+09	0.01	−2.43	1.63E+09	0.00	1.10
124.442	4	26,670	2	108	830,260	1	−1.64	9.86E+09	0.05	−1.43	1.63E+10	0.01	1.08
124.656	4	26,670	2	107	828,875	2	−2.30	2.13E+09	0.01	−2.32	2.05E+09	0.00	1.06
124.809	1	0	4	103	801,225	3	−3.32	2.04E+08	0.00	−3.21	2.70E+08	0.00	0.89
125.305	5	32,210	0	108	830,260	1	−2.18	2.79E+09	0.01	−2.27	2.38E+09	0.00	1.05
125.344	4	26,670	2	106	824,474	3	−2.46	1.46E+09	0.00	−4.78	7.07E+06	0.00	0.82
125.399	7	40,835	4	109	838,289	3	−1.45	1.52E+10	0.04	−1.55	1.21E+10	0.01	0.99
125.683	6	34,610	1	108	830,260	1	−2.58	1.12E+09	0.01	−3.36	1.84E+08	0.00	1.21
125.725	8	42,900	2	109	838,289	3	−2.50	1.32E+09	0.00	−2.52	1.28E+09	0.00	1.12
125.765	1	0	4	101	795,135	3	−3.76	7.31E+07	0.00	−2.91	5.37E+08	0.00	1.17
125.788	2	13,140	2	105	808,130	1	−2.71	8.22E+08	0.00	−2.97	4.67E+08	0.00	1.34
125.903	6	34,610	1	107	828,875	2	−2.64	9.68E+08	0.01	−1.65	9.55E+09	0.01	1.12
126.359	1	0	4	97	791,395	3	−1.43	1.55E+10	0.01	−1.94	4.98E+09	0.00	1.70
126.620	2	13,140	2	104	802,905	2	−2.12	3.17E+09	0.00	−3.42	1.57E+08	0.00	0.58
126.738	1	0	4	96	789,029	5	−1.92	4.95E+09	0.01	−1.78	6.92E+09	0.01	1.04
126.829	1	0	4	95	788,465	3	−1.48	1.37E+10	0.01	−4.30	2.15E+07	0.00	0.38
126.890	2	13,140	2	103	801,225	3	−2.15	2.91E+09	0.01	−2.87	5.75E+08	0.00	0.91
126.952	3	15,205	3	104	802,905	2	−2.12	3.16E+09	0.03	−2.06	3.66E+09	0.00	1.03
127.007	8	42,900	2	108	830,260	1	−1.54	1.19E+10	0.03	−1.33	1.93E+10	0.02	1.00
127.223	3	15,205	3	103	801,225	3	−1.90	5.18E+09	0.02	−1.73	7.84E+09	0.01	1.10
127.231	8	42,900	2	107	828,875	2	−1.31	1.99E+10	0.03	−1.61	1.02E+10	0.01	1.01
127.417	1	0	4	90	784,826	3	−1.95	4.63E+09	0.01	−2.44	1.54E+09	0.00	0.78
127.610	7	40,835	4	106	824,474	3	−0.49	1.33E+11	0.24	−0.41	1.59E+11	0.19	1.05
127.738	2	13,140	2	102	795,995	2	−3.54	1.18E+08	0.00	−2.92	4.89E+08	0.00	0.82
127.878	2	13,140	2	101	795,135	3	−1.97	4.38E+09	0.00	−1.87	5.63E+09	0.01	1.00
127.947	8	42,900	2	106	824,474	3	−1.31	1.98E+10	0.03	−1.28	2.17E+10	0.06	1.02
127.966	4	26,670	2	105	808,130	1	−1.87	5.54E+09	0.02	−1.05	3.76E+10	0.03	1.06

(*continued on next page*)

Table 3 (*continued*)

λ (Å)[a]	Lower Level[b]			Upper Level[b]				HFR			RCI-CV(4p)		
	i	E (cm^{-1})	J	i	E (cm^{-1})	J	log gf	gA (s^{-1})	CF[c]	log gf	gA (s^{-1})	CF[c]	B/C[d]
128.004	2	13,140	2	100	794,365	2	−2.90	5.17E+08	0.00	−3.51	1.25E+08	0.00	1.15
128.075	3	15,205	3	102	795,995	2	−1.48	1.36E+10	0.07	−1.16	2.81E+10	0.03	1.01
128.123	1	0	4	86	780,503	3	−1.67	8.78E+09	0.01	−2.11	3.25E+09	0.00	0.94
128.217	3	15,205	3	101	795,135	3	−1.56	1.12E+10	0.03	−1.54	1.21E+10	0.01	1.09
128.343	3	15,205	3	100	794,365	2	−1.50	1.27E+10	0.06	−1.45	1.43E+10	0.01	1.02
128.425	2	13,140	2	98	791,805	1	−1.45	1.42E+10	0.02	−2.40	1.67E+09	0.00	1.27
128.493	2	13,140	2	97	791,395	3	−4.30	2.01E+07	0.00	−4.90	5.20E+06	0.00	1.99
128.735	1	0	4	84	776,787	4	−4.22	2.43E+07	0.00	−4.72	7.93E+06	0.00	9.12
128.824	1	0	4	83	776,253	3	−1.51	1.24E+10	0.01	−1.57	1.13E+10	0.01	1.13
128.827	4	26,670	2	104	802,905	2	−1.22	2.44E+10	0.03	−1.04	3.64E+10	0.01	1.02
128.834	3	15,205	3	97	791,395	3	−1.17	2.71E+10	0.02	−1.63	9.60E+09	0.00	1.14
128.879	5	32,210	0	105	808,130	1	−2.35	1.78E+09	0.01	−2.23	2.57E+09	0.00	1.07
128.903	1	0	4	82	775,775	4	−1.79	6.45E+09	0.01	−1.35	1.77E+10	0.01	1.07
128.937	1	0	4	81	775,570	3	−1.72	7.69E+09	0.01	−1.30	2.06E+10	0.01	0.96
128.978	2	13,140	2	95	788,465	3	−1.50	1.27E+10	0.01	−2.01	4.03E+09	0.00	1.06
128.990	2	13,140	2	94	788,396	1	−1.42	1.53E+10	0.03	−2.41	1.46E+09	0.00	0.90
129.031	2	13,140	2	93	788,145	2	−2.16	2.76E+09	0.00	−2.27	2.14E+09	0.00	1.12
129.106	4	26,670	2	103	801,225	3	−1.53	1.18E+10	0.04	−1.91	5.06E+09	0.00	1.01
129.155	2	13,140	2	92	787,403	1	−1.62	9.51E+09	0.02	−2.17	2.79E+09	0.00	1.50
129.204	1	0	4	79	773,968	5	−1.32	1.91E+10	0.01	−2.45	1.44E+09	0.00	0.92
129.204	1	0	4	78	773,968	4	−5.19	2.61E+06	0.00	−1.39	1.63E+10	0.01	1.03
129.247	1	0	4	77	773,715	3	−5.57	1.08E+06	0.00	−2.17	2.74E+09	0.00	1.26
129.279	1	0	4	76	773,519	5	−1.95	4.46E+09	0.00	−1.52	1.25E+10	0.03	1.02
129.279	6	34,610	1	105	808,130	1	−2.43	1.49E+09	0.01	−2.81	6.22E+08	0.00	0.86
129.293	2	13,140	2	91	786,580	2	−2.24	2.29E+09	0.00	−2.90	4.98E+08	0.00	1.27
129.305	1	0	4	75	773,363	4	−2.13	2.95E+09	0.00	−3.37	1.76E+08	0.00	4.53
129.323	3	15,205	3	95	788,465	3	−1.62	9.62E+09	0.00	−1.96	4.47E+09	0.00	1.07
129.376	3	15,205	3	93	788,145	2	−1.32	1.93E+10	0.04	−1.12	3.05E+10	0.07	1.05
129.387	1	0	4	73	772,875	4	−1.64	9.08E+09	0.01	−2.07	3.39E+09	0.00	1.31
129.586	2	13,140	2	90	784,826	3	−2.16	2.77E+09	0.00	−2.41	1.58E+09	0.00	0.95
129.639	3	15,205	3	91	786,580	2	−1.05	3.50E+10	0.08	−2.92	4.82E+08	0.00	1.00
129.719	2	13,140	2	89	784,035	1	−2.40	1.60E+09	0.00	−2.26	2.19E+09	0.01	1.05
129.934	3	15,205	3	90	784,826	3	−1.20	2.49E+10	0.01	−1.33	1.89E+10	0.00	1.08
129.984	4	26,670	2	102	795,995	2	−1.31	1.94E+10	0.02	−1.41	1.53E+10	0.01	1.04
130.077	1	0	4	71	768,773	3	−0.82	5.93E+10	0.10	−1.47	1.36E+10	0.01	0.97
130.093	2	13,140	2	88	781,822	2	−2.54	1.13E+09	0.00	−2.29	2.03E+09	0.01	1.07
130.130	4	26,670	2	101	795,135	3	−1.74	7.23E+09	0.01	−1.44	1.47E+10	0.01	1.03
130.158	6	34,610	1	104	802,905	2	−0.82	6.00E+10	0.09	−0.87	5.32E+10	0.04	1.00
130.259	1	0	4	70	767,700	5	−1.79	6.31E+09	0.00	−1.89	5.09E+09	0.00	1.10
130.260	4	26,670	2	100	794,365	2	−2.39	1.60E+09	0.00	−1.18	2.55E+10	0.01	1.07
130.265	2	13,140	2	87	780,805	2	−3.55	1.10E+08	0.00	−2.83	5.74E+08	0.00	6.67
130.316	2	13,140	2	86	780,503	3	−1.97	4.25E+09	0.00	−1.02	3.84E+10	0.02	1.02
130.387	1	0	4	68	766,947	5	−1.94	4.51E+09	0.00	−1.64	8.89E+09	0.01	1.04
130.402	1	0	4	67	766,860	3	−1.67	8.37E+09	0.01	−2.62	9.64E+08	0.00	1.00
130.443	3	15,205	3	88	781,822	2	−0.71	7.72E+10	0.14	−0.78	6.59E+10	0.18	1.03
130.617	3	15,205	3	87	780,805	2	−2.47	1.34E+09	0.00	−3.45	1.37E+08	0.00	0.85
130.668	3	15,205	3	86	780,503	3	−2.33	1.84E+09	0.00	−1.72	7.64E+09	0.00	1.09
130.680	8	42,900	2	105	808,130	1	−2.95	4.36E+08	0.00	−1.79	6.59E+09	0.01	0.94
130.683	2	13,140	2	85	778,350	1	−1.25	2.19E+10	0.03	−1.10	3.13E+10	0.12	1.04
130.696	4	26,670	2	98	791,805	1	−1.97	4.15E+09	0.01	−1.82	6.24E+09	0.01	0.99
130.766	4	26,670	2	97	791,395	3	−2.14	2.82E+09	0.00	−4.28	2.11E+07	0.00	0.57
131.042	2	13,140	2	83	776,253	3	−2.90	4.84E+08	0.00	−1.82	6.07E+09	0.00	1.05
131.050	1	0	4	63	763,070	4	−1.12	2.95E+10	0.06	−1.25	2.20E+10	0.01	0.94
131.160	2	13,140	2	81	775,570	3	−1.22	2.36E+10	0.02	−4.89	5.04E+06	0.00	0.17
131.253	2	13,140	2	80	775,030	1	−1.48	1.27E+10	0.02	−1.36	1.71E+10	0.03	1.04
131.269	4	26,670	2	95	788,465	3	−1.50	1.24E+10	0.01	−3.05	3.52E+08	0.00	1.01
131.281	4	26,670	2	94	788,396	1	−0.85	5.52E+10	0.10	−0.87	4.88E+10	0.03	1.02
131.306	3	15,205	3	84	776,787	4	−2.15	2.73E+09	0.00	−1.92	4.82E+09	0.00	1.07
131.324	4	26,670	2	93	788,145	2	−0.87	5.24E+10	0.07	−1.00	3.84E+10	0.03	1.05
131.340	6	34,610	1	102	795,995	2	−1.04	3.51E+10	0.05	−0.81	5.96E+10	0.14	1.03
131.360	1	0	4	61	761,266	3	−1.20	2.43E+10	0.06	−0.75	7.03E+10	0.12	1.04
131.398	3	15,205	3	83	776,253	3	−0.89	5.01E+10	0.03	−2.05	3.56E+09	0.00	1.29
131.452	4	26,670	2	92	787,403	1	−1.85	5.47E+09	0.01	−3.74	7.27E+07	0.00	2.72
131.479	2	13,140	2	77	773,715	3	−1.72	7.38E+09	0.01	−1.80	6.24E+09	0.00	0.94
131.480	3	15,205	3	82	775,775	4	−1.08	3.18E+10	0.02	−1.69	7.83E+09	0.01	1.05
131.511	7	40,835	4	103	801,225	3	−0.03	3.62E+11	0.44	−2.02	3.75E+09	0.00	1.02
131.516	3	15,205	3	81	775,570	3	−3.46	1.33E+08	0.00	−1.01	3.88E+10	0.01	1.10
131.549	2	13,140	2	74	773,315	2	−2.03	3.57E+09	0.00	−1.89	4.96E+09	0.01	1.13
131.578	8	42,900	2	104	802,905	2	−0.82	5.88E+10	0.05	−1.00	3.84E+10	0.02	1.00
131.595	4	26,670	2	91	786,580	2	−1.38	1.62E+10	0.01	−4.96	4.23E+06	0.00	76.40
131.621	6	34,610	1	100	794,365	2	−1.33	1.81E+10	0.01	−0.88	4.99E+10	0.03	1.04
131.649	5	32,210	0	98	791,805	1	−0.77	6.61E+10	0.13	−1.60	1.04E+10	0.02	1.16
131.707	1	0	4	59	759,260	5	−0.75	6.79E+10	0.12	−0.68	7.97E+10	0.03	1.04
131.733	1	0	4	58	759,110	3	−0.62	9.28E+10	0.11	−4.12	2.96E+07	0.00	0.86

(*continued on next page*)

Table 3 (*continued*)

λ (Å)[a]	Lower Level[b]			Upper Level[b]				HFR			RCI-CV(4p)		
	i	E (cm^{-1})	J	i	E (cm^{-1})	J	log gf	gA (s^{-1})	CF[c]	log gf	gA (s^{-1})	CF[c]	B/C[d]
131.793	3	15,205	3	78	773,968	4	−1.83	5.68E+09	0.00	−1.22	2.32E+10	0.01	1.06
131.837	3	15,205	3	77	773,715	3	−1.87	5.16E+09	0.02	−1.80	6.15E+09	0.00	1.27
131.870	8	42,900	2	103	801,225	3	−0.48	1.28E+11	0.23	−1.74	7.14E+09	0.01	1.09
131.899	3	15,205	3	75	773,363	4	−3.00	3.82E+08	0.00	−3.29	2.01E+08	0.00	0.65
131.899	4	26,670	2	90	784,826	3	−4.07	3.27E+07	0.00	−5.27	2.11E+06	0.00	0.07
131.907	3	15,205	3	74	773,315	2	−1.38	1.61E+10	0.04	−4.49	1.26E+07	0.00	1.18
131.978	6	34,610	1	99	792,311	0	−0.88	5.03E+10	0.16	−1.25	2.29E+10	0.36	1.06
131.984	3	15,205	3	73	772,875	4	−2.73	7.20E+08	0.00	−1.96	4.25E+09	0.00	1.00
132.037	4	26,670	2	89	784,035	1	−2.40	1.54E+09	0.00	−2.06	3.34E+09	0.01	1.06
132.066	6	34,610	1	98	791,805	1	−1.44	1.40E+10	0.04	−2.21	2.45E+09	0.01	1.00
132.243	5	32,210	0	94	788,396	1	−1.24	2.18E+10	0.03	−1.50	1.14E+10	0.05	1.09
132.262	2	13,140	2	72	769,217	2	−1.37	1.61E+10	0.01	−2.08	3.15E+09	0.00	1.69
132.272	1	0	4	55	756,016	4	−1.74	6.93E+09	0.01	−2.93	4.52E+08	0.00	2.87
132.305	1	0	4	54	755,831	4	−0.91	4.66E+10	0.02	−0.77	6.43E+10	0.04	1.01
132.339	2	13,140	2	71	768,773	3	−2.72	7.18E+08	0.00	−1.29	1.97E+10	0.01	1.04
132.416	5	32,210	0	92	787,403	1	−4.24	2.22E+07	0.00	−3.85	5.71E+07	0.00	77.42
132.424	4	26,670	2	88	781,822	2	−1.08	3.13E+10	0.01	−1.94	4.38E+09	0.01	1.00
132.475	1	0	4	53	754,860	3	−0.82	5.75E+10	0.10	−3.25	2.20E+08	0.00	1.48
132.573	7	40,835	4	101	795,135	3	0.10	4.82E+11	0.42	0.11	4.97E+11	0.24	1.02
132.586	2	13,140	2	69	767,369	1	−3.57	1.01E+08	0.00	−3.12	2.85E+08	0.00	0.75
132.602	4	26,670	2	87	780,805	2	−2.00	3.78E+09	0.00	−1.97	4.01E+09	0.00	1.23
132.624	3	15,205	3	72	769,217	2	−1.28	1.98E+10	0.03	−1.99	3.88E+09	0.00	0.97
132.655	4	26,670	2	86	780,503	3	−0.45	1.33E+11	0.06	−3.56	1.08E+08	0.00	0.79
132.664	6	34,610	1	94	788,396	1	−0.74	6.86E+10	0.11	−0.61	8.49E+10	0.13	1.00
132.675	2	13,140	2	67	766,860	3	−2.23	2.21E+09	0.00	−1.97	4.14E+09	0.00	0.99
132.702	3	15,205	3	71	768,773	3	−0.79	6.13E+10	0.10	−1.44	1.40E+10	0.01	1.07
132.708	6	34,610	1	93	788,145	2	−1.24	2.20E+10	0.06	−0.89	4.85E+10	0.10	1.03
132.717	2	13,140	2	66	766,625	2	−2.15	2.67E+09	0.00	−1.35	1.70E+10	0.01	1.04
132.740	1	0	4	50	753,352	5	−1.25	2.13E+10	0.08	−2.61	9.25E+08	0.00	0.92
132.785	8	42,900	2	102	795,995	2	−0.80	5.96E+10	0.05	−0.61	9.21E+10	0.08	1.05
132.839	6	34,610	1	92	787,403	1	−0.81	5.92E+10	0.06	−3.35	1.73E+08	0.00	0.37
132.867	2	13,140	2	64	765,770	1	−1.72	7.13E+09	0.02	−2.36	1.68E+09	0.00	1.28
132.928	1	0	4	49	752,285	4	−0.94	4.37E+10	0.07	−0.83	5.40E+10	0.02	1.04
132.937	8	42,900	2	101	795,135	3	−1.71	7.35E+09	0.01	−0.51	1.19E+11	0.16	1.02
132.969	1	0	4	47	752,054	3	−1.29	1.94E+10	0.03	−0.52	1.17E+11	0.11	1.02
132.984	6	34,610	1	91	786,580	2	−0.34	1.72E+11	0.28	−0.72	7.11E+10	0.07	1.03
132.994	2	13,140	2	64	765,052	2	−1.45	1.32E+10	0.02	−1.32	1.79E+10	0.02	1.01
133.010	5	32,210	0	89	784,035	1	−2.13	2.80E+09	0.01	−1.58	1.03E+10	0.09	1.06
133.035	4	26,670	2	85	778,350	1	−1.42	1.44E+10	0.03	−1.56	1.03E+10	0.02	1.02
133.040	3	15,205	3	67	766,860	3	−1.42	1.43E+10	0.03	−1.42	1.45E+10	0.01	1.12
133.073	8	42,900	2	100	794,365	2	−1.34	1.72E+10	0.01	−1.34	1.71E+10	0.01	0.99
133.081	3	15,205	3	66	766,625	2	−1.21	2.30E+10	0.03	−2.59	9.64E+08	0.00	0.87
133.234	7	40,835	4	97	791,395	3	−1.82	5.65E+09	0.01	−3.80	6.10E+07	0.00	0.70
133.361	3	15,205	3	64	765,052	2	−0.60	9.37E+10	0.28	−0.66	8.19E+10	0.06	1.02
133.408	4	26,670	2	83	776,253	3	−2.35	1.67E+09	0.00	−1.59	9.93E+09	0.00	1.08
133.436	6	34,610	1	89	784,035	1	−1.68	7.86E+09	0.03	−1.29	1.91E+10	0.07	1.02
133.449	1	0	4	45	749,351	3	−3.07	3.16E+08	0.00	−0.62	9.11E+10	0.21	1.03
133.518	2	13,140	2	62	762,105	2	−0.62	8.91E+10	0.07	−0.52	1.12E+11	0.14	1.04
133.528	8	42,900	2	98	791,805	1	−0.42	1.41E+11	0.23	−2.75	6.93E+08	0.00	1.31
133.529	4	26,670	2	81	775,570	3	−2.23	2.21E+09	0.00	−0.42	1.44E+11	0.03	1.03
133.601	8	42,900	2	97	791,395	3	−3.74	6.78E+07	0.00	−1.59	9.76E+09	0.00	1.08
133.626	4	26,670	2	80	775,030	1	−1.50	1.18E+10	0.02	−1.20	2.37E+10	0.04	1.03
133.655	7	40,835	4	96	789,029	5	−0.12	2.82E+11	0.29	−0.07	3.15E+11	0.19	1.04
133.667	2	13,140	2	61	761,266	3	−1.79	6.06E+09	0.01	−4.23	2.23E+07	0.00	2.36
133.714	3	15,205	3	63	763,070	4	−1.27	1.99E+10	0.04	−1.12	2.82E+10	0.01	1.05
133.724	2	13,140	2	60	760,950	1	−2.01	3.67E+09	0.00	−2.88	5.02E+08	0.00	1.14
133.756	7	40,835	4	95	788,465	3	−1.90	4.70E+09	0.00	0.01	3.85E+11	0.38	1.01
133.831	6	34,610	1	88	781,822	2	−1.01	3.61E+10	0.03	−0.87	4.99E+10	0.19	1.00
133.861	4	26,670	2	77	773,715	3	−1.19	2.39E+10	0.05	−0.73	7.12E+10	0.01	1.04
133.887	3	15,205	3	62	762,105	2	−0.92	4.53E+10	0.14	−0.93	4.38E+10	0.08	1.03
133.932	4	26,670	2	74	773,315	2	−0.27	2.02E+11	0.21	−2.22	2.27E+09	0.00	1.08
133.968	1	0	4	42	746,445	3	−1.01	3.63E+10	0.08	−0.70	7.56E+10	0.08	1.04
134.013	6	34,610	1	87	780,805	2	−1.26	2.06E+10	0.01	−3.07	3.14E+08	0.00	0.74
134.023	5	32,210	0	85	778,350	1	−2.58	9.80E+08	0.00	−2.30	1.92E+09	0.02	1.06
134.037	3	15,205	3	61	761,266	3	−0.09	3.01E+11	0.46	−0.91	4.67E+10	0.06	1.00
134.054	2	13,140	2	58	759,110	3	−1.72	7.10E+09	0.02	−3.69	7.75E+07	0.00	1.14
134.091	1	0	4	41	745,762	3	−0.80	5.93E+10	0.03	−2.71	7.37E+08	0.00	0.68
134.126	8	42,900	2	95	788,465	3	−0.68	7.76E+10	0.03	−1.23	2.21E+10	0.02	1.03
134.139	8	42,900	2	94	788,396	1	−2.07	3.15E+09	0.01	−2.33	1.58E+09	0.00	1.01
134.184	8	42,900	2	93	788,145	2	−0.55	1.06E+11	0.13	−0.76	6.44E+10	0.06	1.01
134.193	2	13,140	2	57	758,337	1	−1.74	6.75E+09	0.01	−0.83	5.48E+10	0.06	1.03
134.236	1	0	4	39	744,955	3	0.03	4.00E+11	0.28	−1.88	4.99E+09	0.00	0.98
134.312	1	0	4	38	744,537	4	−0.79	5.97E+10	0.11	−0.92	4.42E+10	0.01	1.00
134.318	8	42,900	2	92	787,403	1	−2.14	2.70E+09	0.01	−1.45	1.34E+10	0.01	1.06

(*continued on next page*)

Table 3 (*continued*)

λ (Å)[a]	Lower Level[b]			Upper Level[b]				HFR			RCI-CV(4p)		
	i	E (cm−1)	J	i	E (cm−1)	J	log gf	gA (s−1)	CF[c]	log gf	gA (s−1)	CF[c]	B/C[d]
134.410	7	40,835	4	90	784,826	3	−2.35	1.64E+09	0.00	−3.49	1.21E+08	0.00	4.81
134.426	3	15,205	3	58	759,110	3	−0.87	4.96E+10	0.09	−1.32	1.81E+10	0.01	1.00
134.456	6	34,610	1	85	778,350	1	−2.03	3.43E+09	0.02	−2.11	2.82E+09	0.01	0.99
134.466	8	42,900	2	91	786,580	2	−1.95	4.14E+09	0.00	−1.95	4.15E+09	0.00	1.03
134.584	2	13,140	2	56	756,170	2	−0.29	1.86E+11	0.28	−0.37	1.59E+11	0.10	1.03
134.622	5	32,210	0	80	775,030	1	−1.17	2.47E+10	0.06	−1.03	3.54E+10	0.20	1.06
134.672	4	26,670	2	72	769,217	2	−0.79	6.01E+10	0.03	−3.12	2.82E+08	0.00	0.99
134.693	1	0	4	36	742,430	5	−2.93	4.29E+08	0.00	−0.78	6.06E+10	0.01	1.04
134.747	9	88,130	0	108	830,260	1	−0.25	2.06E+11	0.53	−0.34	1.76E+11	0.12	1.05
134.752	4	26,670	2	71	768,773	3	−1.14	2.69E+10	0.04	−2.33	1.75E+09	0.00	1.19
134.784	8	42,900	2	90	784,826	3	−2.66	8.04E+08	0.00	−4.03	3.53E+07	0.00	2.44
134.807	1	0	4	35	741,800	3	−2.42	1.39E+09	0.00	−1.02	3.48E+10	0.02	0.97
134.822	2	13,140	2	53	754,860	3	−0.99	3.74E+10	0.06	−4.84	5.41E+06	0.00	0.95
134.843	2	13,140	2	52	754,745	1	−0.40	1.46E+11	0.26	−0.51	1.12E+11	0.07	1.01
134.928	8	42,900	2	89	784,035	1	−0.34	1.67E+11	0.26	−0.26	2.03E+11	0.36	1.02
134.959	3	15,205	3	56	756,170	2	−0.43	1.36E+11	0.42	−4.23	2.17E+07	0.00	1.90
134.987	3	15,205	3	55	756,016	4	0.18	5.61E+11	0.39	−0.11	2.86E+11	0.07	1.05
135.008	4	26,670	2	69	767,369	1	−2.35	1.65E+09	0.00	−0.75	6.44E+10	0.04	1.02
135.016	2	13,140	2	51	753,795	2	−2.33	1.70E+09	0.00	−0.98	3.87E+10	0.01	0.94
135.021	3	15,205	3	54	755,831	4	−0.85	5.16E+10	0.03	−1.31	1.78E+10	0.01	1.05
135.058	6	34,610	1	80	775,030	1	−1.37	1.55E+10	0.03	−1.54	1.04E+10	0.04	1.04
135.072	1	0	4	33	740,348	5	0.24	6.31E+11	0.50	−0.04	3.37E+11	0.07	1.03
135.100	4	26,670	2	67	766,860	3	−0.12	2.76E+11	0.26	−1.28	1.97E+10	0.01	1.05
135.143	4	26,670	2	66	766,625	2	−0.88	4.80E+10	0.02	−0.69	7.44E+10	0.03	1.02
135.196	7	40,835	4	86	780,503	3	−2.23	2.16E+09	0.00	−1.11	2.86E+10	0.01	0.96
135.198	3	15,205	3	53	754,860	3	−0.97	3.88E+10	0.09	−0.22	2.25E+11	0.15	1.03
135.219	1	0	4	32	739,542	4	−0.50	1.14E+11	0.19	−0.77	6.12E+10	0.03	0.99
135.259	1	0	4	31	739,322	3	−0.99	3.70E+10	0.05	−0.93	4.23E+10	0.03	1.03
135.300	4	26,670	2	64	765,770	1	−0.38	1.54E+11	0.31	−1.96	4.03E+09	0.00	0.99
135.315	2	13,140	2	48	752,155	1	−0.57	9.70E+10	0.25	−0.70	7.28E+10	0.17	1.02
135.332	8	42,900	2	88	781,822	2	−0.59	9.31E+10	0.04	−0.31	1.77E+11	0.29	1.02
135.334	2	13,140	2	47	752,054	3	−0.18	2.41E+11	0.21	−1.29	1.88E+10	0.02	1.02
135.372	6	34,610	1	74	773,315	2	−2.59	9.30E+08	0.00	−3.30	1.85E+08	0.00	1.36
135.393	3	15,205	3	51	753,795	2	−0.23	2.15E+11	0.39	−0.87	4.90E+10	0.02	1.02
135.431	4	26,670	2	64	765,052	2	−0.93	4.24E+10	0.06	−1.01	3.52E+10	0.02	1.01
135.456	1	0	4	30	738,248	5	−1.09	2.98E+10	0.02	−2.82	5.44E+08	0.00	1.03
135.519	8	42,900	2	87	780,805	2	−0.71	7.08E+10	0.03	−2.13	2.68E+09	0.00	0.90
135.574	8	42,900	2	86	780,503	3	−0.50	1.14E+11	0.07	−0.57	9.89E+10	0.04	1.05
135.614	1	0	4	29	737,388	4	−0.05	3.20E+11	0.22	0.12	4.76E+11	0.24	1.03
135.617	2	13,140	2	46	750,512	2	−1.02	3.42E+10	0.06	−3.26	1.99E+08	0.00	1.39
135.670	3	15,205	3	49	752,285	4	−2.56	1.00E+09	0.00	−1.80	5.63E+09	0.00	1.01
135.713	3	15,205	3	47	752,054	3	−1.13	2.69E+10	0.03	−1.54	1.06E+10	0.01	0.99
135.831	2	13,140	2	45	749,351	3	−2.08	2.97E+09	0.00	−0.88	4.85E+10	0.12	1.02
135.855	1	0	4	28	736,077	5	−1.49	1.16E+10	0.01	−1.85	5.14E+09	0.00	1.14
135.878	7	40,835	4	84	776,787	4	−0.67	7.68E+10	0.05	−1.89	4.75E+09	0.00	1.31
135.961	2	13,140	2	44	748,644	1	−1.56	9.89E+09	0.01	−1.29	1.83E+10	0.01	0.96
135.971	8	42,900	2	85	778,350	1	−2.31	1.76E+09	0.00	−3.34	1.65E+08	0.00	1.23
135.974	4	26,670	2	62	762,105	2	−1.55	1.02E+10	0.02	−1.59	9.16E+09	0.01	1.01
135.977	7	40,835	4	83	776,253	3	−1.71	7.10E+09	0.00	−1.70	7.39E+09	0.00	1.15
135.998	3	15,205	3	46	750,512	2	−0.58	9.54E+10	0.20	−0.48	1.19E+11	0.08	1.02
136.009	1	0	4	27	735,246	4	−0.82	5.50E+10	0.04	−2.02	3.42E+09	0.00	0.92
136.025	5	32,210	0	69	767,369	1	−0.67	7.72E+10	0.31	−1.07	3.17E+10	0.24	1.02
136.066	7	40,835	4	82	775,775	4	−0.44	1.31E+11	0.15	−1.48	1.17E+10	0.01	1.03
136.103	7	40,835	4	81	775,570	3	−2.36	1.59E+09	0.00	−1.55	1.03E+10	0.00	0.77
136.127	6	34,610	1	72	769,217	2	−1.74	6.58E+09	0.01	−2.60	9.00E+08	0.00	1.68
136.129	4	26,670	2	61	761,266	3	−3.22	2.15E+08	0.00	−0.86	5.01E+10	0.04	1.03
136.188	4	26,670	2	60	760,950	1	−0.78	5.92E+10	0.03	−0.49	1.19E+11	0.13	1.02
136.213	3	15,205	3	45	749,351	3	−0.11	2.79E+11	0.15	−0.71	7.17E+10	0.11	1.02
136.285	1	0	4	26	733,755	3	−0.47	1.21E+11	0.16	−0.82	5.36E+10	0.01	0.94
136.322	5	32,210	0	64	765,770	1	−0.98	3.79E+10	0.12	−1.45	1.34E+10	0.05	1.24
136.349	2	13,140	2	43	746,552	2	−0.45	1.29E+11	0.16	−0.99	3.66E+10	0.03	1.04
136.360	8	42,900	2	83	776,253	3	−1.03	3.36E+10	0.02	−1.01	3.65E+10	0.01	1.01
136.369	2	13,140	2	42	746,445	3	−1.67	7.66E+09	0.01	−0.19	2.35E+11	0.18	1.04
136.401	7	40,835	4	79	773,968	5	−0.58	9.54E+10	0.07	0.19	5.60E+11	0.18	1.02
136.401	7	40,835	4	78	773,968	4	0.15	5.07E+11	0.33	−0.41	1.38E+11	0.06	1.02
136.448	7	40,835	4	77	773,715	3	−0.34	1.66E+11	0.56	−3.61	8.91E+07	0.00	6.22
136.471	6	34,610	1	69	767,369	1	−1.54	1.02E+10	0.04	−2.87	4.77E+08	0.00	1.01
136.484	7	40,835	4	76	773,519	5	−0.72	6.84E+10	0.02	−2.52	1.09E+09	0.00	2.69
136.487	8	42,900	2	81	775,570	3	−1.39	1.47E+10	0.01	−0.93	4.26E+10	0.01	1.18
136.496	2	13,140	2	41	745,762	3	−3.16	2.48E+08	0.00	−1.20	2.28E+10	0.01	0.99
136.514	7	40,835	4	75	773,363	4	−0.36	1.57E+11	0.15	−4.18	2.42E+07	0.00	0.33
136.530	4	26,670	2	58	759,110	3	−1.76	6.27E+09	0.01	−0.27	1.98E+11	0.07	1.04
136.550	2	13,140	2	40	745,470	1	−0.54	1.04E+11	0.20	−0.73	6.56E+10	0.04	1.03
136.588	8	42,900	2	80	775,030	1	−0.60	9.03E+10	0.15	−0.71	7.04E+10	0.12	1.02

(*continued on next page*)

Table 3 (*continued*)

λ (Å)[a]	Lower Level[b]			Upper Level[b]				HFR			RCI-CV(4p)		
	i	E (cm^{-1})	J	i	E (cm^{-1})	J	log gf	gA (s^{-1})	CF[c]	log gf	gA (s^{-1})	CF[c]	B/C[d]
136.605	7	40,835	4	73	772,875	4	−0.14	2.56E+11	0.19	−2.32	1.71E+09	0.00	0.99
136.609	6	34,610	1	66	766,625	2	−1.03	3.32E+10	0.03	−1.10	2.85E+10	0.03	1.07
136.647	2	13,140	2	39	744,955	3	−1.62	8.53E+09	0.01	−2.31	1.78E+09	0.00	1.15
136.674	4	26,670	2	57	758,337	1	−0.58	9.41E+10	0.06	−0.80	5.63E+10	0.05	1.01
136.713	1	0	4	25	731,458	4	0.08	4.30E+11	0.42	−0.35	1.58E+11	0.05	1.02
136.734	3	15,205	3	43	746,552	2	−1.12	2.72E+10	0.14	−0.53	1.07E+11	0.12	1.00
136.754	3	15,205	3	42	746,445	3	−1.79	5.78E+09	0.01	−1.72	6.88E+09	0.01	1.08
136.769	6	34,610	1	64	765,770	1	−2.65	7.95E+08	0.00	−1.79	5.81E+09	0.01	1.10
136.834	8	42,900	2	77	773,715	3	−0.40	1.41E+11	0.19	−0.68	7.61E+10	0.02	0.94
136.882	3	15,205	3	41	745,762	3	−1.67	7.60E+09	0.00	−1.82	5.50E+09	0.00	0.69
136.903	6	34,610	1	64	765,052	2	−1.73	6.62E+09	0.02	−1.56	9.73E+09	0.01	0.87
136.908	8	42,900	2	74	773,315	2	−0.58	9.31E+10	0.11	−1.14	2.59E+10	0.02	1.02
136.922	1	0	4	24	730,345	5	−1.20	2.24E+10	0.06	−1.44	1.28E+10	0.01	1.03
136.942	1	0	4	23	730,235	4	−1.37	1.52E+10	0.04	−1.87	4.73E+09	0.00	1.52
137.033	3	15,205	3	39	744,955	3	−1.13	2.64E+10	0.02	−0.13	2.66E+11	0.19	1.03
137.080	4	26,670	2	56	756,170	2	−2.00	3.51E+09	0.01	−2.45	1.26E+09	0.00	1.09
137.089	2	13,140	2	37	742,594	1	−4.23	2.09E+07	0.00	−2.55	9.93E+08	0.00	1.12
137.112	3	15,205	3	38	744,537	4	−1.57	9.59E+09	0.02	−2.70	7.05E+08	0.00	0.99
137.223	5	32,210	0	60	760,950	1	−1.45	1.27E+10	0.02	−0.83	5.55E+10	0.37	1.06
137.238	2	13,140	2	35	741,800	3	−0.36	1.54E+11	0.16	−0.64	8.08E+10	0.05	0.99
137.327	4	26,670	2	53	754,860	3	−2.16	2.45E+09	0.00	−2.79	5.87E+08	0.00	1.22
137.348	4	26,670	2	52	754,745	1	−2.94	4.07E+08	0.00	−1.68	7.39E+09	0.01	0.92
137.374	7	40,835	4	71	768,773	3	−1.50	1.12E+10	0.12	−2.36	1.56E+09	0.00	1.05
137.435	2	13,140	2	34	740,757	2	−1.11	2.76E+10	0.04	−0.47	1.21E+11	0.19	1.02
137.458	6	34,610	1	62	762,105	2	−3.34	1.61E+08	0.00	−3.66	7.64E+07	0.00	1.16
137.528	4	26,670	2	51	753,795	2	−1.85	4.94E+09	0.01	−1.90	4.46E+09	0.00	1.05
137.577	7	40,835	4	70	767,700	5	−0.83	5.18E+10	0.02	−2.14	2.52E+09	0.00	0.77
137.628	3	15,205	3	35	741,800	3	−2.52	1.08E+09	0.00	−1.73	6.56E+09	0.00	1.05
137.677	6	34,610	1	60	760,950	1	−0.73	6.47E+10	0.07	−1.80	5.59E+09	0.03	1.02
137.681	8	42,900	2	72	769,217	2	−3.70	7.00E+07	0.00	−1.75	6.22E+09	0.00	1.19
137.707	2	13,140	2	31	739,322	3	−1.49	1.13E+10	0.01	−1.79	5.65E+09	0.00	0.94
137.717	5	32,210	0	57	758,337	1	−2.05	3.15E+09	0.01	−2.30	1.84E+09	0.01	0.98
137.720	7	40,835	4	68	766,947	5	−0.72	6.64E+10	0.03	−0.55	9.91E+10	0.19	1.03
137.736	7	40,835	4	67	766,860	3	−2.06	3.07E+09	0.03	−0.44	1.30E+11	0.11	1.03
137.765	8	42,900	2	71	768,773	3	−3.90	4.38E+07	0.00	−1.03	3.31E+10	0.01	1.06
137.774	1	0	4	22	725,825	3	−0.42	1.33E+11	0.14	−0.63	8.30E+10	0.04	1.01
137.826	3	15,205	3	34	740,757	2	−3.02	3.34E+08	0.00	−1.13	2.62E+10	0.04	1.01
137.839	4	26,670	2	48	752,155	1	−3.20	2.21E+08	0.00	−3.49	1.12E+08	0.00	0.97
137.858	4	26,670	2	47	752,054	3	−1.30	1.77E+10	0.02	−1.96	3.89E+09	0.00	1.03
137.921	1	0	4	21	725,053	4	−1.02	3.34E+10	0.03	−0.69	7.09E+10	0.03	1.05
138.032	8	42,900	2	69	767,369	1	−1.57	9.37E+09	0.02	−1.67	7.54E+09	0.01	0.98
138.057	3	15,205	3	32	739,542	4	−2.38	1.45E+09	0.01	−2.14	2.50E+09	0.00	1.05
138.099	3	15,205	3	31	739,322	3	−1.98	3.68E+09	0.00	−2.25	1.95E+09	0.00	0.95
138.129	8	42,900	2	67	766,860	3	−1.56	9.58E+09	0.02	−0.30	1.78E+11	0.12	1.02
138.152	4	26,670	2	46	750,512	2	−0.55	9.82E+10	0.16	−1.68	7.36E+09	0.00	0.99
138.174	6	34,610	1	57	758,337	1	−0.56	9.65E+10	0.11	−0.85	4.92E+10	0.12	1.03
138.174	8	42,900	2	66	766,625	2	−3.15	2.45E+08	0.00	−4.26	1.90E+07	0.00	7.55
138.337	8	42,900	2	64	765,770	1	−1.89	4.49E+09	0.01	−5.49	1.13E+06	0.00	0.09
138.374	4	26,670	2	45	749,351	3	−1.97	3.73E+09	0.00	−1.87	4.75E+09	0.01	1.01
138.402	5	32,210	0	52	754,745	1	−2.47	1.17E+09	0.01	−1.39	1.46E+10	0.04	1.02
138.420	1	0	4	20	722,439	5	−1.04	3.20E+10	0.14	−1.02	3.27E+10	0.03	1.03
138.459	7	40,835	4	63	763,070	4	−0.26	1.91E+11	0.44	−0.47	1.18E+11	0.02	1.03
138.469	3	15,205	3	29	737,388	4	−1.25	1.97E+10	0.03	−1.22	2.10E+10	0.03	1.00
138.475	8	42,900	2	64	765,052	2	−3.78	5.75E+07	0.00	−4.20	2.16E+07	0.00	1.78
138.509	4	26,670	2	44	748,644	1	−6.91	4.29E+04	0.00	−2.59	8.83E+08	0.00	1.19
138.589	6	34,610	1	56	756,170	2	−2.79	5.66E+08	0.00	−2.82	5.31E+08	0.00	1.23
138.770	2	13,140	2	26	733,755	3	−0.71	6.75E+10	0.08	−1.05	3.09E+10	0.01	1.06
138.806	7	40,835	4	61	761,266	3	−1.98	3.63E+09	0.04	−1.80	5.53E+09	0.01	0.98
138.863	6	34,610	1	52	754,745	1	−2.44	1.25E+09	0.01	−1.63	8.07E+09	0.03	1.04
138.881	3	15,205	3	27	735,246	4	−2.39	1.41E+09	0.00	−2.24	2.00E+09	0.00	1.07
138.889	9	88,130	0	105	808,130	1	−1.11	2.66E+10	0.16	−0.86	5.20E+10	0.07	1.17
138.899	5	32,210	0	48	752,155	1	−0.90	4.36E+10	0.15	−0.92	4.32E+10	0.32	1.05
138.912	4	26,670	2	43	746,552	2	−3.39	1.42E+08	0.00	−0.60	8.69E+10	0.07	1.02
138.932	4	26,670	2	42	746,445	3	−2.90	4.32E+08	0.00	−1.85	4.96E+09	0.00	0.99
139.042	8	42,900	2	62	762,105	2	−1.33	1.63E+10	0.02	−1.67	7.39E+09	0.01	1.02
139.046	6	34,610	1	51	753,795	2	−0.45	1.21E+11	0.28	−3.02	3.28E+08	0.00	0.54
139.064	4	26,670	2	41	745,762	3	−1.57	9.22E+09	0.01	−2.89	4.47E+08	0.00	1.24
139.121	4	26,670	2	40	745,470	1	−1.80	5.43E+09	0.01	−2.00	3.44E+09	0.00	0.94
139.169	3	15,205	3	26	733,755	3	−1.19	2.20E+10	0.03	−1.69	7.03E+09	0.00	0.97
139.193	7	40,835	4	59	759,260	5	−0.56	9.48E+10	0.22	−0.79	5.55E+10	0.02	1.03
139.205	8	42,900	2	61	761,266	3	−1.53	1.01E+10	0.03	−5.60	8.88E+05	0.00	0.25
139.221	4	26,670	2	39	744,955	3	−1.07	2.92E+10	0.04	−1.70	6.88E+09	0.01	1.06
139.222	7	40,835	4	58	759,110	3	−1.64	7.84E+09	0.08	−2.27	1.90E+09	0.00	0.95
139.266	8	42,900	2	60	760,950	1	−2.29	1.75E+09	0.00	−1.79	5.62E+09	0.01	1.04

(*continued on next page*)

Table 3 (*continued*)

λ (Å)[a]	Lower Level[b]			Upper Level[b]				HFR			RCI-CV(4p)		
	i	E (cm−1)	J	i	E (cm−1)	J	log gf	gA (s^{-1})	CF[c]	log gf	gA (s^{-1})	CF[c]	B/C[d]
139.364	6	34,610	1	48	752,155	1	−2.00	3.47E+09	0.01	−1.73	6.29E+09	0.02	1.03
139.406	1	0	4	18	717,330	3	−2.87	4.63E+08	0.00	−2.36	1.45E+09	0.00	0.60
139.580	5	32,210	0	44	748,644	1	−2.83	5.06E+08	0.00	−1.94	3.98E+09	0.01	0.87
139.615	3	15,205	3	25	731,458	4	−2.88	4.48E+08	0.00	−3.23	1.99E+08	0.00	1.03
139.624	8	42,900	2	58	759,110	3	−3.65	7.72E+07	0.00	−2.05	3.14E+09	0.00	1.14
139.680	4	26,670	2	37	742,594	1	−2.05	3.08E+09	0.01	−2.12	2.59E+09	0.00	1.01
139.684	6	34,610	1	46	750,512	2	−0.93	3.98E+10	0.11	−0.56	9.46E+10	0.10	0.97
139.775	8	42,900	2	57	758,337	1	−2.45	1.20E+09	0.00	−2.37	1.47E+09	0.00	1.30
139.825	7	40,835	4	55	756,016	4	−1.33	1.61E+10	0.10	−1.98	3.54E+09	0.00	0.98
139.835	4	26,670	2	35	741,800	3	−1.10	2.70E+10	0.04	−0.80	5.34E+10	0.02	0.98
139.854	3	15,205	3	23	730,235	4	−4.34	1.56E+07	0.00	−2.47	1.15E+09	0.00	0.99
139.861	7	40,835	4	54	755,831	4	−1.55	9.59E+09	0.01	−1.40	1.36E+10	0.01	0.97
139.889	1	0	4	16	714,855	3	−1.96	3.76E+09	0.01	−2.26	1.87E+09	0.00	1.00
140.039	4	26,670	2	34	740,757	2	−1.43	1.26E+10	0.02	−1.73	6.40E+09	0.01	1.06
140.049	6	34,610	1	44	748,644	1	−5.25	1.94E+06	0.00	−3.70	6.65E+07	0.00	5.12
140.051	7	40,835	4	53	754,860	3	−2.28	1.79E+09	0.02	−4.25	1.96E+07	0.00	6.43
140.199	8	42,900	2	56	756,170	2	−1.51	1.04E+10	0.02	−1.68	7.13E+09	0.01	0.97
140.201	5	32,210	0	40	745,470	1	−1.21	2.09E+10	0.07	−1.46	1.21E+10	0.04	1.19
140.314	2	13,140	2	22	725,825	3	−1.53	9.98E+09	0.02	−1.61	8.24E+09	0.00	0.98
140.321	4	26,670	2	31	739,322	3	−2.68	7.10E+08	0.00	−2.33	1.57E+09	0.00	1.03
140.348	7	40,835	4	50	753,352	5	−1.27	1.82E+10	0.18	−1.47	1.14E+10	0.00	1.09
140.405	1	0	4	15	712,223	4	−1.12	2.55E+10	0.11	−1.64	7.74E+09	0.00	0.95
140.457	8	42,900	2	53	754,860	3	−2.09	2.76E+09	0.01	−1.73	6.38E+09	0.00	0.89
140.461	6	34,610	1	43	746,552	2	−2.00	3.36E+09	0.01	−1.05	3.05E+10	0.04	1.02
140.480	8	42,900	2	52	754,745	1	−1.83	5.04E+09	0.01	−2.03	3.15E+09	0.00	0.77
140.558	7	40,835	4	49	752,285	4	−1.91	4.18E+09	0.02	−2.86	4.50E+08	0.00	1.63
140.604	7	40,835	4	47	752,054	3	−1.48	1.11E+10	0.02	−1.73	6.40E+09	0.01	1.05
140.668	8	42,900	2	51	753,795	2	−2.41	1.30E+09	0.00	−1.85	4.80E+09	0.00	0.93
140.675	6	34,610	1	40	745,470	1	−1.85	4.76E+09	0.01	−1.70	6.68E+09	0.01	1.06
140.722	3	15,205	3	22	725,825	3	−1.82	5.15E+09	0.01	−2.18	2.21E+09	0.00	1.00
140.769	5	32,210	0	37	742,594	1	−2.35	1.52E+09	0.01	−2.19	2.26E+09	0.02	1.22
140.875	3	15,205	3	21	725,053	4	−3.16	2.32E+08	0.00	−2.16	2.34E+09	0.00	1.07
140.987	1	0	4	14	709,285	3	−1.43	1.25E+10	0.09	−1.61	8.17E+09	0.01	1.02
140.993	8	42,900	2	48	752,155	1	−1.96	3.70E+09	0.01	−1.95	3.75E+09	0.02	1.05
141.013	8	42,900	2	47	752,054	3	−1.95	3.80E+09	0.00	−3.96	3.73E+07	0.00	0.73
141.140	7	40,835	4	45	749,351	3	−2.07	2.88E+09	0.01	−2.56	9.26E+08	0.00	1.08
141.246	6	34,610	1	37	742,594	1	−1.20	2.13E+10	0.09	−1.32	1.60E+10	0.01	0.97
141.271	2	13,140	2	19	721,001	2	−1.51	1.04E+10	0.01	−2.31	1.62E+09	0.00	0.92
141.320	8	42,900	2	46	750,512	2	−2.52	1.01E+09	0.00	−2.31	1.65E+09	0.00	0.96
141.426	4	26,670	2	26	733,755	3	−1.20	2.11E+10	0.02	−1.70	6.60E+09	0.00	0.88
141.553	8	42,900	2	45	749,351	3	−1.71	6.53E+09	0.01	−3.54	9.72E+07	0.00	1.51
141.614	6	34,610	1	34	740,757	2	−1.90	4.19E+09	0.01	−2.08	2.81E+09	0.01	0.94
141.684	3	15,205	3	19	721,001	2	−3.62	8.08E+07	0.00	−3.67	7.05E+07	0.00	0.96
141.694	8	42,900	2	44	748,644	1	−5.35	1.50E+06	0.00	−3.66	7.15E+07	0.00	161.82
141.721	7	40,835	4	42	746,445	3	−2.83	4.86E+08	0.00	−1.35	1.49E+10	0.02	0.97
141.859	7	40,835	4	41	745,762	3	−3.15	2.32E+08	0.00	−3.46	1.15E+08	0.00	53.89
142.007	2	13,140	2	18	717,330	3	−3.00	3.30E+08	0.00	−3.54	9.25E+07	0.00	0.20
142.021	7	40,835	4	39	744,955	3	−2.10	2.62E+09	0.00	−3.03	3.14E+08	0.00	0.66
142.106	7	40,835	4	38	744,537	4	−3.71	6.47E+07	0.00	−4.29	1.66E+07	0.00	2.20
142.111	9	88,130	0	98	791,805	1	−1.06	2.88E+10	0.13	−1.21	2.20E+10	0.04	1.00
142.116	8	42,900	2	43	746,552	2	−3.80	5.21E+07	0.00	−2.17	2.22E+09	0.00	1.03
142.137	8	42,900	2	42	746,445	3	−2.95	3.68E+08	0.00	−2.29	1.72E+09	0.00	0.88
142.275	8	42,900	2	41	745,762	3	−1.78	5.51E+09	0.00	−1.96	3.64E+09	0.00	1.37
142.331	2	13,140	2	17	715,730	2	−1.75	5.83E+09	0.01	−1.84	4.81E+09	0.00	0.99
142.335	8	42,900	2	40	745,470	1	−1.96	3.58E+09	0.01	−1.76	5.74E+09	0.00	0.89
142.425	3	15,205	3	18	717,330	3	−2.94	3.74E+08	0.00	−2.76	5.45E+08	0.00	0.89
142.439	8	42,900	2	39	744,955	3	−1.68	6.84E+09	0.01	−1.52	9.90E+09	0.02	1.00
142.508	2	13,140	2	16	714,855	3	−1.99	3.34E+09	0.01	−2.24	1.86E+09	0.00	1.04
142.532	7	40,835	4	36	742,430	5	−4.33	1.52E+07	0.00	−2.56	8.93E+08	0.00	1.00
142.660	7	40,835	4	35	741,800	3	−1.57	8.89E+09	0.04	−1.74	5.97E+09	0.00	1.07
142.750	3	15,205	3	17	715,730	2	−1.54	9.50E+09	0.02	−3.19	2.11E+08	0.00	1.10
142.803	9	88,130	0	94	788,396	1	−2.06	2.82E+09	0.02	−5.92	3.70E+05	0.00	0.39
142.920	8	42,900	2	37	742,594	1	−3.05	2.91E+08	0.00	−2.76	5.68E+08	0.00	0.59
142.929	3	15,205	3	16	714,855	3	−1.44	1.19E+10	0.02	−1.46	1.13E+10	0.01	0.99
142.957	7	40,835	4	33	740,348	5	−2.27	1.76E+09	0.01	−2.91	3.99E+08	0.00	0.93
143.006	9	88,130	0	92	787,403	1	−2.49	1.06E+09	0.01	−4.52	1.06E+07	0.00	0.95
143.030	4	26,670	2	22	725,825	3	−1.29	1.68E+10	0.03	−1.42	1.22E+10	0.00	1.01
143.082	8	42,900	2	35	741,800	3	−2.29	1.68E+09	0.00	−5.62	7.75E+05	0.00	4.92
143.122	7	40,835	4	32	739,542	4	−2.68	6.80E+08	0.00	−3.01	3.13E+08	0.00	0.64
143.167	7	40,835	4	31	739,322	3	−4.41	1.27E+07	0.00	−4.01	3.18E+07	0.00	8.20
143.296	8	42,900	2	34	740,757	2	−2.59	8.38E+08	0.00	−4.28	1.72E+07	0.00	0.77
143.387	7	40,835	4	30	738,248	5	−3.20	2.06E+08	0.00	−3.42	1.20E+08	0.00	1.12
143.468	3	15,205	3	15	712,223	4	−2.96	3.57E+08	0.00	−2.84	4.62E+08	0.00	1.10
143.564	7	40,835	4	29	737,388	4	−3.57	8.67E+07	0.00	−2.60	8.00E+08	0.00	0.96

(*continued on next page*)

Table 3 (*continued*)

λ (Å)[a]	Lower Level[b]			Upper Level[b]				HFR			RCI-CV(4p)		
	i	E (cm^{-1})	J	i	E (cm^{-1})	J	log gf	gA (s^{-1})	CF[c]	log gf	gA (s^{-1})	CF[c]	B/C[d]
143.591	8	42,900	2	31	739,322	3	−1.71	6.26E+09	0.01	−1.77	5.44E+09	0.01	0.94
143.648	2	13,140	2	14	709,285	3	−2.59	8.33E+08	0.01	−2.75	5.70E+08	0.00	0.96
143.698	9	88,130	0	89	784,035	1	−1.58	8.47E+09	0.12	−1.61	8.24E+09	0.07	1.02
143.807	1	0	4	13	695,376	4	−1.45	1.14E+10	0.03	−1.50	1.02E+10	0.03	0.99
143.835	7	40,835	4	28	736,077	5	−5.00	3.20E+06	0.00	−2.24	1.85E+09	0.00	0.99
144.007	7	40,835	4	27	735,246	4	−3.43	1.20E+08	0.00	−2.88	4.23E+08	0.00	1.49
144.024	4	26,670	2	19	721,001	2	−2.38	1.33E+09	0.00	−3.63	7.53E+07	0.00	2.00
144.076	3	15,205	3	14	709,285	3	−2.23	1.90E+09	0.01	−2.26	1.75E+09	0.01	0.99
144.317	7	40,835	4	26	733,755	3	−3.88	4.26E+07	0.00	−4.72	5.97E+06	0.00	0.02
144.748	8	42,900	2	26	733,755	3	−1.95	3.61E+09	0.01	−1.91	3.84E+09	0.00	0.77
144.789	4	26,670	2	18	717,330	3	−2.98	3.31E+08	0.00	−3.57	8.17E+07	0.00	0.46
144.797	7	40,835	4	25	731,458	4	−2.34	1.44E+09	0.01	−2.39	1.28E+09	0.00	0.95
144.881	9	88,130	0	85	778,350	1	−2.15	2.27E+09	0.05	−2.06	2.85E+09	0.05	1.05
145.031	7	40,835	4	24	730,345	5	−1.83	4.68E+09	0.05	−1.90	3.94E+09	0.01	1.00
145.054	7	40,835	4	23	730,235	4	−3.48	1.05E+08	0.00	−3.69	6.38E+07	0.00	21.77
145.125	4	26,670	2	17	715,730	2	−2.88	4.21E+08	0.00	−2.40	1.28E+09	0.00	0.98
145.310	4	26,670	2	16	714,855	3	−3.71	6.12E+07	0.00	−3.13	2.31E+08	0.00	1.02
145.556	1	0	4	12	687,020	4	−1.47	1.06E+10	0.00	−1.38	1.25E+10	0.00	0.97
145.582	9	88,130	0	80	775,030	1	−2.04	2.87E+09	0.06	−2.07	2.77E+09	0.02	1.00
145.690	6	34,610	1	19	721,001	2	−4.61	7.72E+06	0.00	−7.65	6.94E+03	0.00	0.00
145.988	7	40,835	4	22	725,825	3	−4.54	9.11E+06	0.00	−3.93	3.63E+07	0.00	1.94
146.152	7	40,835	4	21	725,053	4	−2.23	1.83E+09	0.01	−2.45	1.09E+09	0.00	0.94
146.429	8	42,900	2	22	725,825	3	−2.34	1.43E+09	0.00	−2.36	1.35E+09	0.00	1.01
146.495	4	26,670	2	14	709,285	3	−2.04	2.83E+09	0.02	−2.05	2.71E+09	0.01	0.98
146.713	7	40,835	4	20	722,439	5	−2.42	1.18E+09	0.04	−2.61	7.44E+08	0.00	1.01
146.817	6	34,610	1	17	715,730	2	−1.82	4.63E+09	0.02	−2.54	8.81E+08	0.00	0.75
147.022	3	15,205	3	13	695,376	4	−2.69	6.33E+08	0.01	−2.67	6.55E+08	0.01	0.96
147.151	1	0	4	10	679,572	3	−1.28	1.62E+10	0.00	−1.15	2.07E+10	0.00	1.50
147.224	9	88,130	0	69	767,369	1	−4.41	1.20E+07	0.00	−4.84	4.61E+06	0.00	2.33
147.471	8	42,900	2	19	721,001	2	−3.52	9.23E+07	0.00	−4.46	1.04E+07	0.00	0.62
147.571	9	88,130	0	64	765,770	1	−3.04	2.83E+08	0.01	−3.90	4.04E+07	0.00	1.21
147.821	7	40,835	4	18	717,330	3	−1.42	1.16E+10	0.01	−1.16	2.03E+10	0.00	1.36
148.273	8	42,900	2	18	717,330	3	−3.45	1.08E+08	0.00	−3.34	1.34E+08	0.00	75.44
148.364	7	40,835	4	16	714,855	3	−2.79	4.87E+08	0.00	−2.72	5.70E+08	0.00	1.54
148.626	8	42,900	2	17	715,730	2	−2.95	3.36E+08	0.00	−3.80	4.80E+07	0.00	1.11
148.628	9	88,130	0	60	760,950	1	−4.78	5.06E+06	0.00	−3.48	1.05E+08	0.00	0.99
148.819	8	42,900	2	16	714,855	3	−3.40	1.20E+08	0.00	−3.96	3.28E+07	0.00	1.91
148.851	3	15,205	3	12	687,020	4	−2.44	1.08E+09	0.00	−2.54	8.22E+08	0.00	0.99
148.945	7	40,835	4	15	712,223	4	−3.62	7.25E+07	0.00	−3.88	3.92E+07	0.00	0.68
149.208	9	88,130	0	57	758,337	1	−3.41	1.17E+08	0.00	−2.60	7.85E+08	0.00	1.10
149.600	7	40,835	4	14	709,285	3	−3.99	3.02E+07	0.00	−3.55	8.35E+07	0.00	1.33
149.727	2	13,140	2	11	681,023	2	−1.49	9.66E+09	0.01	−1.49	9.12E+09	0.00	0.88
150.012	9	88,130	0	52	754,745	1	−2.46	1.02E+09	0.03	−3.85	4.37E+07	0.00	0.70
150.053	2	13,140	2	10	679,572	3	−2.81	4.54E+08	0.00	−2.65	6.30E+08	0.00	3.81
150.063	8	42,900	2	14	709,285	3	−3.46	1.02E+08	0.00	−3.26	1.62E+08	0.00	1.07
150.191	3	15,205	3	11	681,023	2	−4.51	9.04E+06	0.00	−4.26	1.53E+07	0.00	0.29
150.519	3	15,205	3	10	679,572	3	−4.21	1.84E+07	0.00	−4.49	9.15E+06	0.00	0.08
150.597	9	88,130	0	48	752,155	1	−2.77	5.03E+08	0.01	−3.55	8.41E+07	0.00	1.09
151.397	9	88,130	0	44	748,644	1	−3.91	3.59E+07	0.00	−4.96	3.23E+06	0.00	0.67
152.128	9	88,130	0	40	745,470	1	−3.03	2.72E+08	0.01	−3.05	2.65E+08	0.00	0.77
152.779	7	40,835	4	13	695,376	4	−3.36	1.26E+08	0.00	−3.42	1.08E+08	0.00	0.96
152.797	9	88,130	0	37	742,594	1	−3.62	6.80E+07	0.00	−6.98	3.07E+04	0.00	0.02
152.823	4	26,670	2	11	681,023	2	−2.18	1.90E+09	0.00	−2.15	1.91E+09	0.00	1.18
153.162	4	26,670	2	10	679,572	3	−2.56	7.92E+08	0.00	−2.38	1.12E+09	0.00	4.84
154.700	6	34,610	1	11	681,023	2	−2.26	1.54E+09	0.01	−2.34	1.21E+09	0.00	1.08
154.754	7	40,835	4	12	687,020	4	−2.68	5.78E+08	0.01	−2.90	3.32E+08	0.00	0.98
156.559	7	40,835	4	10	679,572	3	−2.08	2.29E+09	0.01	−2.37	1.10E+09	0.00	1.27
156.710	8	42,900	2	11	681,023	2	−3.07	2.32E+08	0.00	−2.94	2.94E+08	0.00	0.24
157.067	8	42,900	2	10	679,572	3	−2.61	6.67E+08	0.00	−2.53	7.63E+08	0.00	1.76

[a] Ritz wavelengths computed using the experimental energy level values of [7].
[b] Experimental energy levels from [7].
[c] Cancellation factor (see text).
[d] Ratio between the line strengths calculated using the Babushkin (B) and the Coulomb (C) gauges (see text).

ratio <gf(RCI-V(6f))/gf(RCI-V(5f))> is equal to 1.01 ± 0.12. In that respect, one can be also confident that the main valence correlation effects were considered in our RCI-CV(4p) model.

Churilov et al. [7] computed the transition probabilities of the $4d^8-(4d^75p+4d^74f+4p^54d^9)$ transitions using the HFR method with a more restricted CI expansion than ours, i.e. they considered the interaction between $4d^8$, $4d^75s$ and $4d^65s^2$ in the even parity and between $4d^7np$ ($n=5,6$), $4d^7nf$ ($n=4-6$) and $4p^54d^9$ in the odd parity. In Figs. 4 and 5, the gA-values of Churilov et al. [7] are compared with those obtained by, respectively, our HFR and RCI-CV(4p) models excluding from the comparison the lines with strong cancellation effects and/or bad gauges agreement. One can see from Fig. 4 that our extended CI expansion does not significantly change the transition rates, the average ratio <gA

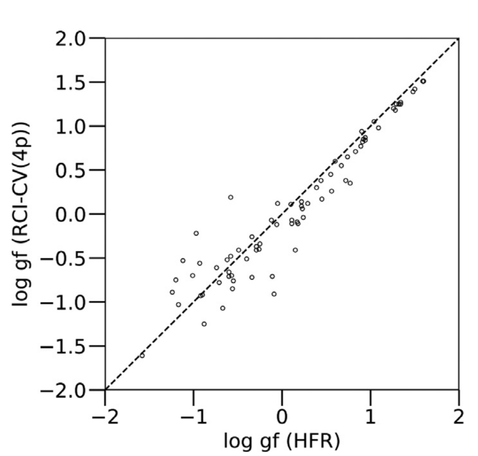

Fig. 1. Comparison between the log gf-values obtained in the present work with our RCI-CV(4p) and HFR models for Xe XI spectral lines. Lines with weak cancellation effects (CF>0.05) and good gauges agreements (0.9 < B/C < 1.1) have been selected.

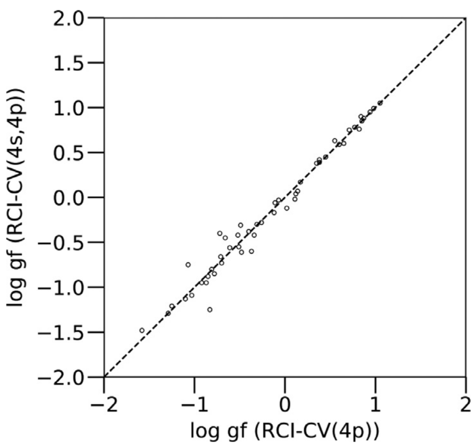

Fig. 2. Comparison between the log gf-values obtained in the present work with our RCI-CV(4 s,4p) and RCI-CV(4p) models for Xe XI spectral lines. Lines with weak cancellation effects (CF>0.05) and good gauges agreements (0.9 < B/C < 1.1) have been selected.

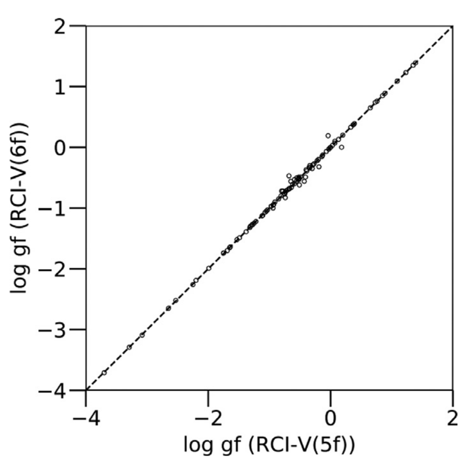

Fig. 3. Comparison between the log gf-values obtained in the present work with our RCI-V(5f) and RCI-V(6f) models for Xe XI spectral lines. Lines with weak cancellation effects (CF>0.05) and good gauges agreements (0.9 < B/C < 1.1) have been selected.

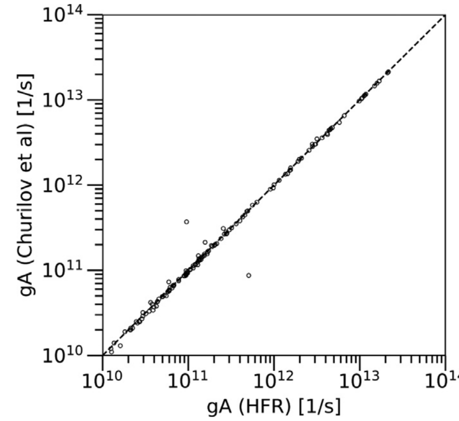

Fig. 4. Comparison between the gA-values obtained in the present work with our HFR model and those published by Churilov et al. [7] for Xe XI spectral lines. Lines with weak cancellation effects (CF>0.05) have been selected.

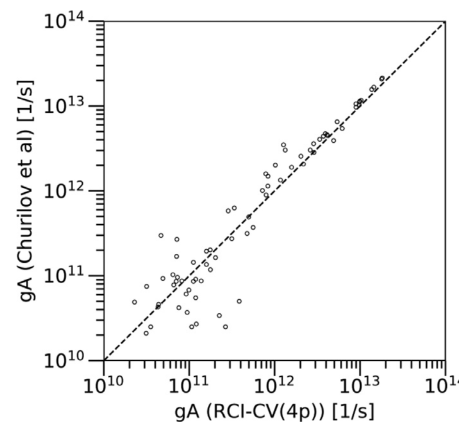

Fig. 5. Comparison between the gA-values obtained in the present work with our RCI-CV(4p) model and those published by Churilov et al. [7] for Xe XI spectral lines. Lines with weak cancellation effects (CF>0.05) and good gauges agreements (0.9 < B/C < 1.1) have been selected.

[7]/gA(HFR)> being equal to 1.00 ± 0.02. It is therefore not surprising that Fig. 5 looks similar than Fig. 1 where our HFR and RCI-CV(4p) log gf-values are compared.

Here again, a 20% systematic decrease of the rates is observed due to missing 4p subshell core-excited configurations. For the strong lines (gA > 10^{12} s^{-1}), the average ratio <gA [7]/gA(RCI-CV(4p))> is in fact equal to 1.25 ± 0.41.

Finally, the FAC transition rates of Shen et al. [8] have been compared with our values for the 31 strong lines reported in their Table B and used to assess their accuracy. The average rate ratios are equal to 0.89 ± 0.26 with our HFR model and 1.41 ± 0.94 with our RCI-CV(4p) model, i.e. the rates of [8] appear thus to be systematically about 10% smaller than our HFR values and ∼40% greater than our RCI-CV(4p) values although the standard deviation of the latter ratios is quite high (∼95%). Here, also, the lines affected by strong cancellation effects or/and strong gauges disagreements have been excluded from the comparisons. Unfortunately, the authors did not estimate any cancellation factors nor the gauges agreements of their FAC line strengths. These accuracy indicators could have explained the significant standard deviation of the rate ratios with respect to RCI-CV(4p). The large systematics with our RCI-CV(4p) model is again mainly the consequence of missing 4p subshell single, double and triple core-holes configurations in their CI expansion. The small one with our HFR model is probably due to the fact that they considered only the correlations up to the shell with principal quantum number $n = 5$. In that respect, their accuracy estimate of the FAC rates being better than 20% [8] seems rather optimistic.

4. Conclusion

Two independent atomic structure computation methods, i.e. the *ab initio* MCDHF/RCI and semi-empirical HFR methods, have been used to determine the oscillator strengths and the transition probabilities of 576 electric dipole transitions of Xe XI falling in the EUV spectral range 102 Å–157 Å. Among these E1 lines, about 500 have their MCDHF/RCI or/and HFR line strengths affected by strong cancellation effects due to the strong mixing of the atomic states or/and their MCDHF/RCI transition rates show strong disagreements between the gauges.

Finally, it has been found that the core-excitation effects caused by the inclusion of single to triple 4p-holes configurations in the CI expansion decrease systematically the transition rates by 20%. Further opening of the core shells does not change the latter.

Acknowledgements

PP and PQ are respectively Research Director and Research Associate of the Belgian Fund for Scientific Research F.R.S.-FNRS. Financial support from this organization is gratefully acknowledged. EBM is grateful to Belgian colleagues for their hospitality during his stay at Université de Mons – UMONS. SEY was supported by Marien Ngouabi University from Congo.

References

[1] Abramov IS, Gospodchikov ED, Shalashov AG. Extreme-ultraviolet light source for lithography based on an expanding jet of dense xenon plasma supported by microwaves. Phys Rev Appl 2018;10:034065.
[2] Chkhalo NI, Salashchenko NN. Next generation nanolithography based on Ru/Be and Rh/Sr multilayer optics. AIP Adv 2013;3:082130.
[3] Milora SL, Houlberg WA, Lengyel LL, Mertens V. Pellet fuelling. Nucl Fus 1995;35:657.
[4] Reznichenko PV, Vinyar IV, Kuteev BV. An injector of xenon macroscopic pellets for quenching the fusion reaction in a tokamak. Tech Phys 2000;45:174.
[5] Beiersdorfer P. Highly charged ions in magnetic fusion plasmas: research opportunities and diagnostic necessities. J Phys B 2015;48:144017.
[6] Churilov S, Joshi YN, Reader J. High-Resolution spectrum of xenon ions at 13.4 nm. Opt Lett 2003;28:1478.
[7] Churilov SS, Joshi YN, Reader J, Kildiyarova RR. $4p^6 4d^8 - (4d^7 5p + 4d^7 4f + 4p^5 4d^9)$ transitions in Xe XI. Phys. Scr. 2004;70:126.
[8] Shen Y, Gao C, Zeng J. Electron impact collision strengths and transition rates for extreme ultraviolet emission from Xe^{10+}. At Data Nucl Data Tables 2009;95:1.
[9] Gu MF. The flexible atomic Code. Can J Phys 2008;86:675.
[10] Grant IP. Relativistic quantum theory of atoms and molecules. Theory and computation. New York: Springer; 2007.
[11] Jönsson P, Gaigalas G, Bieron J, Froese Fischer C, Grant IP. New version: GRASP2K relativistic atomic structure package. Comput Phys Commun 2013;184:2197.
[12] Froese Fischer C, Godefroid MR, Brage T, Jönsson P, Gaigalas G. Advanced multiconfiguration methods for complex atoms: I. Energies and wave function. J Phys B 2016;49:182004.
[13] Carette T, Drag C, Scharf O, Blondel C, Delsart C, Froese Fischer C, Godefroid MR. Isotope shift in the sulfur electron Affinity: Observation and theory. Phys. Rev. A 2010;81:042522.
[14] Cowan RD. The theory of atomic structure and spectra. Berkeley: University of California Press; 1981.
[15] Zhang W, Palmeri P, Quinet P, É Biémont. Transition probabilities in te II and te III spectra. Astron. Astrophys. 2013;551:A136.